2015

Impact of Multileaf Collimator Configuration Parameters on the Dosimetric Accuracy of 6-Mv Intensity-Modulated Radiation Therapy Treatment Plans

Nicholas Colin Petersen
Louisiana State University and Agricultural and Mechanical College

IMPACT OF MULTILEAF COLLIMATOR CONFIGURATION PARAMETERS ON THE DOSIMETRIC ACCURACY OF 6-MV INTENSITY-MODULATED RADIATION THERAPY TREATMENT PLANS

A Thesis

Submitted to the Graduate Faculty of the
Louisiana State University and
Agricultural and Mechanical College
in partial fulfillment of the
requirements for the degree of
Master of Science

in

The Department of Physics and Astronomy

by
Nicholas Colin Petersen
B.S., Oregon State University, 2012
August 2015

Acknowledgements

I would like to thank Dr. Rui Zhang, my advisor, for all the hard work he has done to guide this project through to completion. I am also very appreciative to the rest of my advisory committee for their support and feedback: Wayne Newhauser, David Perrin, Dan Neck, Geoff Clayton, and Rob Hynes. I'd like to give a special thanks to David Perrin, who has helped me on this project tremendously through its various iterations. I would also like to thank Dr John Gibbons, who helped get me started.

Thanks to my fellow classmates for the comradery and emotional support over the last several years: Ryan Schurr, Hatim Chafi, Colie Woods, Paul Maggi, and Will Donahue. I'll miss you all. Thanks also to Mary Bird Perkins residents Margaret Hernandez, Tony Mazza, Ben Rusk, and Adam Watts.

Thanks to MBPCC dosimetry staff for showing me the ropes of treatment planning and the laughs: Frank Apollo, Hamlet Spears, Eddie Singleton, and Chad Dunn. Thanks also to the MBPCC therapy staff for the help. Thanks to Elekta service engineer James Payne for teaching me the ins and outs of the Elekta Synergy linac.

Thanks to LSU and MBPCC administrative staff who have helped with so much over the years: Susan Hammond, Paige Barcia, Katie Bailey, and Farrar Tingle.

Finally, thanks to my parents, Marcia and Rich, and my brother Curtis, who have all given me so much support.

Table of Contents

List of Tables

List of Figures

Abstract

Purpose: To improve the dosimetric accuracy of intensity modulated radiation therapy (IMRT) dose distributions as calculated by the treatment planning system (TPS) by optimizing the parameters that govern multileaf collimator (MLC) transmission and rounded leaf offset.

Methods: The MLC leaf transmission was optimized based on measurements made with ionization chambers and radiographic film. The rounded leaf offset table was optimized by measuring the radiation field edge as a function of leaf bank position with an ionization chamber in a water scanning tank and comparing the location to TPS equivalent dose calculations. Optimizations were validated by performing IMRT quality assurance (QA) tests on 19 gantry-static IMRT plans. Planar dose measurements were performed with film and a planar diode array and compared to TPS calculated dose distributions with default and optimized parameters.

Results: Based on measurements, the leaf transmission factor was changed from a default value of 0.001 to 0.005. This optimization resulted in a statistically significant worsening of IMRT QA gamma index passing rate, because the currently used model is already slightly higher than the measured data originally used to commission the machine. The rounded leaf offset table had little room for improvement, with the average difference between the default and optimized offset values being -0.2 ± 0.7 mm. This reflects the excellent leaf position calibration protocol of physics staff.

Conclusion: The hypothesis that TPS dosimetric accuracy of IMRT fields could be improved by optimizing the rounded leaf offset table and MLC transmission parameters was not supported by the results of this work.

Chapter 1: Introduction

1.1.External Beam Radiation Therapy

1.1.1.IMRT

The goal of external beam radiation cancer therapy is to deliver a tumoricidal dose to the planning treatment volume while minimizing dose to healthy tissue and critical structures. In most cases, the field size of the desired therapeutic beam is much smaller than the x-ray field generated by the linear accelerator. Collimators are used to shape the therapeutic beam by attenuating unwanted out-of-field radiation down to an acceptable level.

Intensity Modulated Radiation Therapy (IMRT) is now one of the most common treatment modalities for external beam radiation therapy. IMRT can deliver highly conformal dose distributions in the patient, allowing for the escalation of dose in the treatment volume while simultaneously improving the sparing of healthy tissue and critical structures surrounding the target (Ezzell et al., 2003). This is achieved with a complex radiation fluence from the treatment head. The most common way to deliver this complex radiation fluence is by delivering many subfields collimated to different shapes such that the cumulative fluence from all subfields will approach the desired dose distribution in the patient. Depending on the plan, there could be many different subfields with greatly varying shapes. IMRT is typically delivered with a 6 MV beam due to its desirable depth dose profile, reduced scatter dose, and lack of photoneutrons when compared to higher beam energies.

Many tumors are located deep within the patient anatomy, meaning there can be significant entrance dose from photons that are absorbed in the patient's healthy tissue before reaching the target. Since x-rays are attenuated exponentially, there can also be a significant amount of exit dose from photons which are transmitted through the target without being completely absorbed. To mitigate these factors, external beam photon therapy usually consists of multiple beams incident on the patient at various angles. This provides many more degrees of freedom for treatment planning and provides more control over dose distributions in the patient. Multiple beams can spread out the unwanted entrance and exit doses to lower the dose to healthy tissue and critical structures while still maintaining an adequate dose distribution in the target volume.

Volumetric Modulated Arc Therapy (VMAT) is a commonly used type of IMRT in which the gantry rotates around the patient while the beam is continuously delivering dose. Typically, treatments comprise of multiple arcs that each cover a full 360°. Additionally, VMAT allows continuous variations in dose rate, collimated field shape, and gantry rotation speed. All of these variable settings help conform dose distributions throughout the patient's anatomy or increase the speed of the treatment delivery. For many cases, VMAT is often much faster than conventional IMRT and allows for a greater patient workload on a single machine. Henceforward, the term "IMRT" will refer to both conventional (gantry-static) IMRT as well as VMAT type therapies.

1.1.2.Multileaf Collimator (MLC) Systems

Before IMRT became a widespread treatment modality, a single field with a complex shape would usually be collimated with a custom molded or machined block. This type of collimation is unsuitable for IMRT because the custom blocks for the many different subfields would be expensive and time consuming to produce. Additionally, swapping blocks from the tray would make treatment delivery time prohibitively long. The multileaf collimator (MLC) system was designed to overcome these limitations and make IMRT treatments feasible (Boyer et al., 2001). A MLC consists of two opposing banks of many thin, computer controlled high density metal slabs referred to as “leaves” (Figure 1.1). Each leaf can move forward and backward independently to give the two edges of the field an irregular shape. The ubiquity of MLC systems on modern linacs has largely supplanted the use of cerrobend blocks for photon treatments.

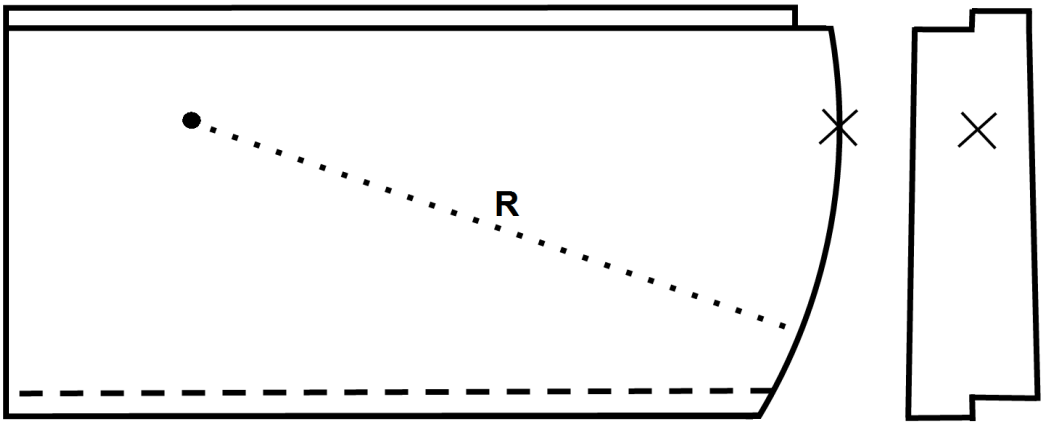

Figure 1.1: Side and front views of the Elekta MLCi2 leaf. The radius of curvature of the leaf end is denoted with R. The tip of the leaf (i.e. the furthest forward point of the rounded leaf end) is denoted with the X. Notice that the leaf tip is located closer to the top of the leaf than the bottom, and that the top and bottom of the leaf have split levels. Not to scale.

1.1.3.Treatment Planning System (TPS)

Computer technology has also greatly enhanced the planning and delivery of radiation therapy. External beam radiotherapy treatment plans are created on a treatment planning system (TPS). Prior to planning, the relevant portion of the patient's body is scanned and their anatomy is reconstructed in three dimensions via computed tomography (CT). Since the image is generated with x-rays, each voxel contains information about how x-rays will propagate through it. During the planning phase, these CT images are used to simulate how the beams will distribute dose throughout the patient. A conventional (non-IMRT) radiotherapy plan will generally use forward planning. This is essentially a guess-and-check system, where beams are set up and the user can change various parameters to achieve an acceptable dose distribution. The planner can change things such as field size, beam energy, wedge use, SSD, beam weighting, etc. in order to improve the plan's performance.

1.1.4.Inverse Planning

The forward planning method does not work for IMRT treatments because there could potentially be thousands of field shapes to optimize, too many for a human user. Instead, inverse planning is used. Rather than specifying beam parameters, the planner specifies various goals of the treatment, including maximum or minimum dose to a specified region of interest, maximum or minimum dose to a percentage of a specified region of interest, and others. The user can also choose how to weight their goals. The TPS iteratively searches for the optimum machine settings which results in a dose distribution in the patient

that satisfies the goals specified by the user. Once the TPS has this radiation fluence, it then converts it into a deliverable plan, using the characteristics of the linac used to the deliver the beam.

In order for the TPS to convert the desired radiation fluence into a deliverable plan, the linac must be properly characterized in the TPS. A large amount of data is used to commission a machine in a TPS system, including information about the collimators which shape the beam. This includes the physical dimensions and shape of the leaves in the MLC, details about how radiation is transmitted through the MLC and the jaws, and the mechanical limits of MLC leaf motion.

1.2.MLC Transmission

1.2.1.X-ray Attenuation

The purpose of any collimator in radiotherapy is to shape the radiation field into the desired shape by attenuating unwanted radiation. This is achieved by placing a sufficient amount of attenuating material between the radiation source and the patient. The proportion of incident radiation fluence that remains after passing through a given material is known as the transmission factor. For photon radiation, to a first order approximation the transmission is governed by an exponential, or

$$T = \exp(-\mu \cdot \ell) \qquad 1.1$$

where μ (with units of inverse-length) represents the linear attenuation coefficient for a specific material and photon energy and ℓ represents the path length of the photon through the material. Note that Equation 1.1 is for “good geometry,”

where radiation scattered in the collimator never reaches the detector. In reality, there is a buildup factor which accounts for the extra scatter. This factor would be generally be determined experimentally. For linear accelerator dose calculations, one contributor to the scattered radiation dose is referred to as the “collimator scatter factor” or more generally S_C. The S_C factor is dependent on beam energy, wedge presence, and field size, and is measured during beam commissioning.

The linear attenuation coefficient, μ, has a strong energy dependence. The primary photon interactions are the photoelectric effect (which is most likely to occur with lower energy photons), Compton scatter (which is most likely to occur with intermediate energy photons), and pair production (which is most likely to occur with higher energy photons). A photon of any given energy will have a certain probability of these interactions occurring per unit path length of travel through any given material, characterized by μ.

Calculating transmission through an MLC requires knowledge of the energy spectrum of the beam. Linear accelerators generate x-rays by impinging high energy electrons upon a tungsten target, which generates x-rays via bremsstrahlung interactions. A bremsstrahlung x-ray will have some portion of the incident electron’s energy but not all of it. Lower energy x-rays are proportionally more likely to be generated via bremsstrahlung interactions. However, lower energy x-rays are more strongly attenuated when passing through the flattening filter. The result is a complicated energy spectrum, an example of which can be seen in Figure 1.2.

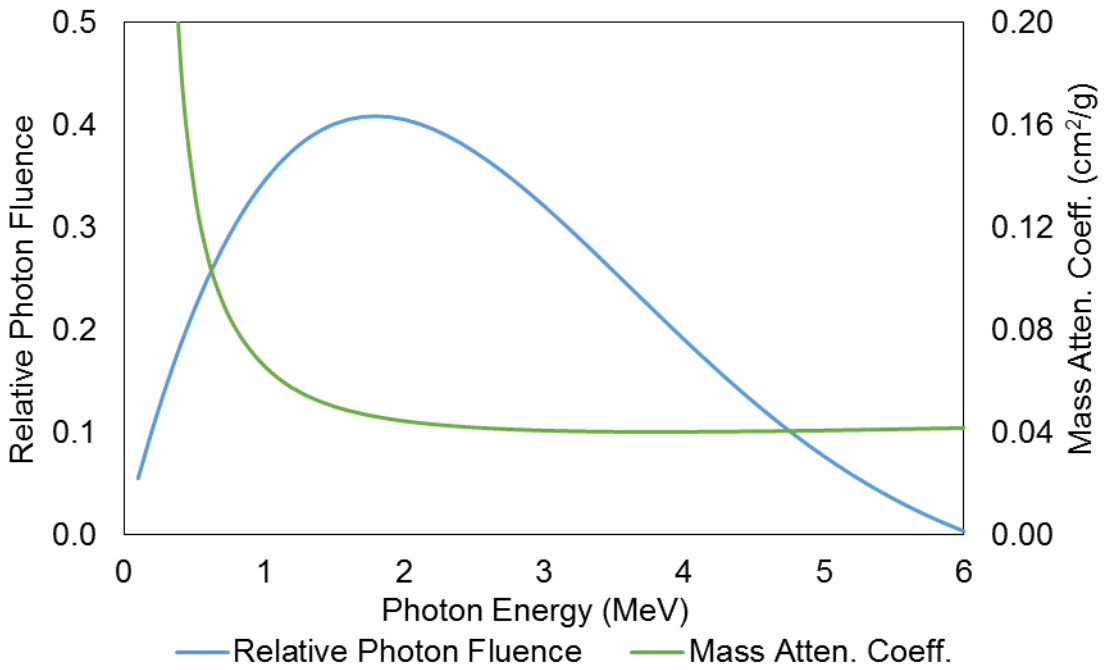

Figure 1.2: Relative photon fluence and mass attenuation coefficient as functions of energy. The relative number of photons is from the Pinnacle[3] TPS, based on models from the literature (Mohan, Chui, & Lidofsky, 1985). It represents the beam energy spectrum after it has been transmitted through the flattening filter, which has hardened the beam by preferentially removing low energy photons with high attenuation coefficients. The mass attenuation coefficients are for x-rays in a 95% tungsten alloy and come from NIST (Berger et al., 2009).

1.2.2.Leaf Transmission

The leaf transmission parameter in a treatment planning system refers to the amount of radiation that is transmitted through the full thickness of the leaf. While this value could be calculated from the leaf thickness, leaf material composition, and beam energy spectrum, it is typically measured experimentally, for the reasons described in Section 1.2.1. The Elekta MLCi2 (Elekta Corporation, Stockholm, Sweden) leaves have a thickness of 8.2 cm of a tungsten alloy (Orton, 2006), which consists of 95% tungsten, 3.4% nickel, and 1.6% iron (Boyer et al., 2001), and has a mass density of 18.0 g/cm^3 (Orton, 2006). The average photon energy in a 6 MV beam is about 2 MeV. A 2 MeV

beam would be attenuated down to around 0.14%, based on attenuation data from NIST (Berger et al., 2009). However, this monoenergetic calculation neglects the other photon energies present in the beam (up to 6 MeV), which may have lower attenuation coefficients, and also neglects beam hardening. Beam hardening occurs when a polyenergetic beam is attenuated by a material. Photons with higher attenuation coefficients are more likely to be absorbed in the material, leaving the remaining photons that are less likely to be absorbed or scattered. Indeed, the energy spectrum shown in Figure 1.2 has already been hardened by the target and the flattening filter. These are parts of the treatment head that the beam must travel through. Beam hardening will result in a higher transmission through the leaf than would otherwise be expected.

1.2.3.Interleaf Leakage

Because the leaves move independently of one another, there is a small space between each leaf, called the interleaf gap, where there is no material present to attenuate radiation. Most MLC systems (but not all) have a tongue-and-groove to intercept radiation incident between to leaves (Boyer et al., 2001). The tongue-and-groove consists of an irregular side shape such that radiation incident on the leaf gap does not have an unimpeded path through the MLC. Different vendors offer different types of tongue-and-groove designs, examples can be seen in Figure 1.3

The Elekta MLCi2, however, does not use a tongue-and-groove design. The sides of each leaf are flat and lie flat against one another. Instead of relying

on a tongue-and-groove to block interleaf leakage, the MLCi2 has two alternative features: a backup jaw and an unfocused shape.

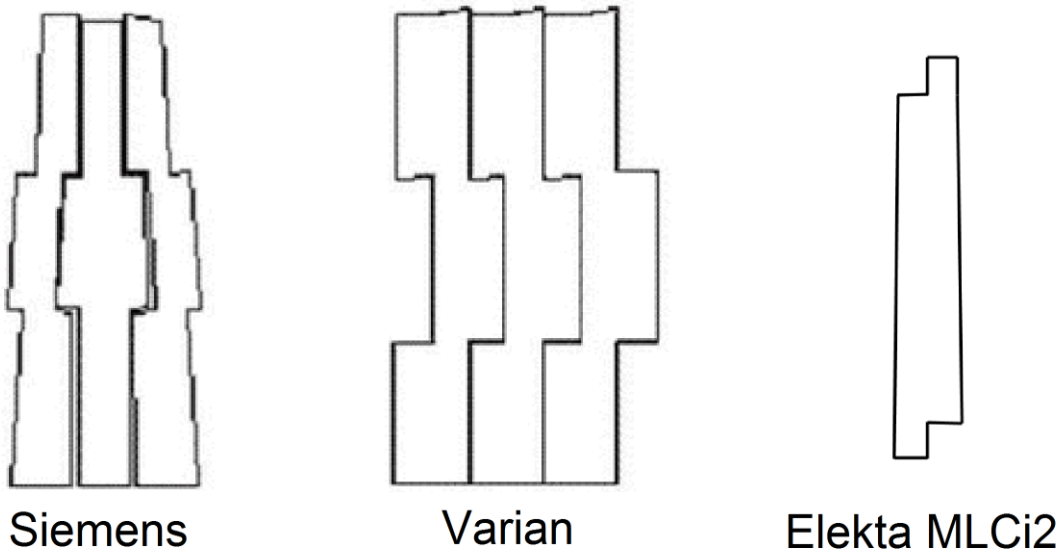

Figure 1.3: Leaf designs from various vendors. The figures representing Siemens and Varian designs come from Hariri & Shahriari (2010), while the Elekta MLCi2 figure is based on the design by Orton (2006).

The unfocused shape refers to the fact that the sides of the leaves do not follow the divergence of the source. This means that the interleaf gap is parallel to the rays emanating from the radiation source, so no radiation can travel directly through the gap without being passing through the leaf. However, they do have similar divergence, so there is still less attenuation for x-rays that travel mostly through the interleaf space. The sides of the leaves are focused on a point near to but not coincident with the radiation source (Payne, 2015).

The backup jaw refers to a solid slab of tungsten alloy that sits underneath each leaf bank. The backup jaw is so-called because it is thinner than the other set of jaws (3 cm thick versus 7.8 cm thick). This is because most of the collimation is provided by the MLC system. The backup jaw tracks the leaf

motion and will automatically position itself so that it is located 0.1 cm behind the most retracted leaf. The backup jaw provides additional attenuation in general and also will attenuate interleaf leakage. For a complicated field shaped by the leaves (Figure 1.4), there could be a large difference between individual leaf positions, which could result in a large are of the field that is blocked by the leaves but not the backup jaw. In this case, the interleaf leakage will only be mitigated by the fact that the sides of the leaves have a different divergence of the radiation source, and there could still be a significant amount of interleaf leakage in these areas. According to the international standards set forth by the International Electrotechnical Commission, leakage radiation through parts of an MLC should not exceed 5 % of the maximum absorbed dose at the maximum depth dose at the center of a 10 cm x 10 cm square radiation field ("Particular requirements for the safety of electron accelerators in the range 1 MeV to 50 MeV," 1998).

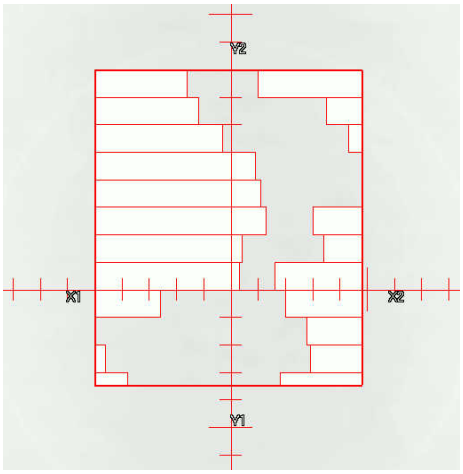

Figure 1.4: MLC leaf positions (light red lines) and jaw positions (bold red lines). The white blocks represent leaves in the MLC. The white areas are blocked by MLC only, and interleaf leakage will not be blocked by the backup jaw.

1.3.Leaf Offset

1.3.1.Rounded Leaf Ends

Most commercial MLC systems are designed so that the leaves all move in the same plane, meaning they don't match the divergence of the radiation source, referred to as "unfocused" (Boyer et al., 2001). The unfocused leaf design is simpler to engineer than one in which the leaf moves perpendicular to the divergence of the beam, but the downside is that the radiation's angle of incidence on the end of the leaf is dependent on the leaf position. Unfocused leaves are designed with a rounded end, making the radiation penumbra size relatively consistent for all leaf positions. Without rounded ends, the penumbra would be very small if the leaf was positioned along the central axis, and very large if the leaf was retracted far from the central axis (Boyer et al., 2001).

There are generally three different ways to describe the position of a leaf, all of which are projected to the isocentric plane: the light field position, the radiation field position, and the leaf tip position (Vial et al., 2006) (Figure 1.5).The light field position corresponds to position of the ray that is tangent to the rounded end of the leaf and therefore corresponds to the visible light emitted from the treatment head, which has the same divergence as the radiation source (Vial et al., 2006). The radiation field position refers to the point at which the radiation beam is attenuated by some factor, usually 50% (Vial et al., 2006). The leaf tip position refers to the physical tip of the leaf extended to the isocentric plane (Vial et al., 2006). All three of these leaf position descriptors depend on the

angle of incidence of radiation from the source and therefore also depend on leaf position.

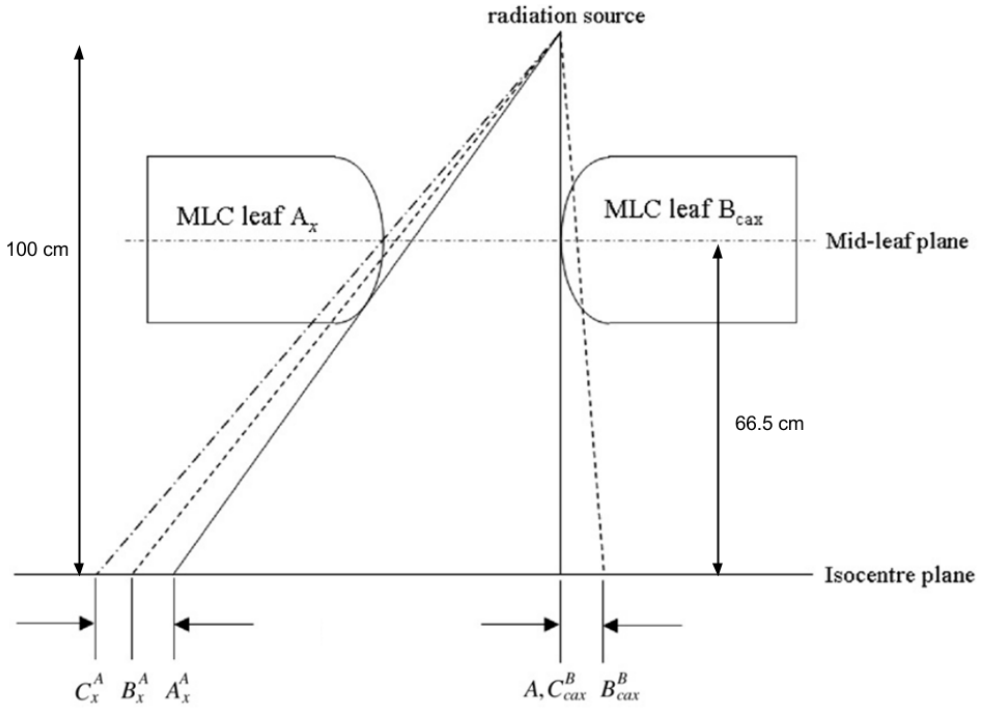

Figure 1.5: Diagram showing rounded leaf offset from Vial et al. (2006). Point C represents the projected leaf tip position, Point B represents the projected radiation field edge position, and Point A represents the projected light field position. The difference between points A and C represents the light field offset, and the difference between points B and C represent the radiation field offset.

1.3.2.Leaf Offset Table

It is conventional for the user to specify the position of the leaf using the leaf tip position. However, depending on where the leaf is positioned, the radiation attenuation at the leaf tip position could vary greatly. The radiation incident at the tips position could be attenuated by nearly the full thickness of the leaf or it could be attenuated by nothing at all, depending on the angle of incidence. For this reason, the leaf tip position is not ideal to define the edge of the field. It is instead recommended to use a leaf offset table (Ezzell et al., 2003).

The leaf offset table shifts the leaf slightly so that the edge of the field is not defined by the leaf tip position, but by either the light field position or the radiation field position. The light field offset table is the difference between the light field position and the leaf tip position as a function of leaf tip position, while the radiation field offset table is the difference between the radiation field position and the leaf tip position. Either table can be used. It is generally simpler to use the light field position, because the position of the light field as a function of leaf position can easily be measured visually by moving the leaf banks to various field sizes and marking the linacs light field position on a piece of graph paper. Measuring the location of the radiation field is more complicated, because it depends on collimator scatter, phantom scatter, and radiation measurement conditions. For example, the edge of the radiation field might appear to be located in a different location if it's measured at d_{max} or at a different depth. In addition, Pinnacle^3 TPS has only one offset table for all photon beam energies. In reality, the radiation field offset will differ between the different photon beam energies of the machine.

The Elekta Synergy linear accelerator is controlled with Elekta Integrity V1.2 software. According to Elekta, the linac software does have a built-in offset table that shifts the actual mechanical leaf tip positions so that the edge of the radiation field is coincident with the user-defined edge of the field. However, the software does not allow the user to edit or view the list. Specific information from the manufacturer was not available, e.g. how the offset table is applied, what the table contains, or whether the table is a light-field offset table or a radiation-field

offset table. Different facilities may use different protocols to calibrate the leaf positions, which could alter the efficacy of Elekta's internal offset table. Furthermore, since the internal offset table can only be edited by Elekta personnel, a clinic cannot set the offset table to correspond to a light-field offset or radiation-field offset.

1.4.Hypothesis

1.4.1.Motivation

Mary Bird Perkins Cancer Center (MBPCC) has five Elekta Synergy linear accelerators equipped with the MLCi2 model treatment heads at MBPCC four satellite locations. Characteristics of the MLC system can be seen in Table 1.1. All five of these linacs have matched data sets so that treatments should be delivered identically between them. MBPCC uses the Philips Pinnacle^3 treatment planning system (Philips Medical Systems, Andover, MA) for all external beam radiation treatments delivered from these linacs.

Table 1.1: Elekta MLCi2 characteristics. The projected dimensions are projected from the source to the isocentric plane (100 cm from the source).

Number of leaves:	40 per bank (80 total)
Leaf width (projected):	1 cm
Leaf thickness:	8.2 cm
Tip radius:	15 cm
Composition (by mass):	95% W, 3.4% Ni, 1.6% Fe
Source to (bottom of) MLC:	37.7 cm
Physical density:	18.0 g/cm^3
Range of motion (projected):	32.5 cm

When the first Elekta Synergy was originally commissioned at MBPCC, the MLC leaf banks were calibrated to best match Pinnacle^3 field size calculations based on the default offset table in the TPS (Perrin & Neck, 2015).

The linac has a limited capability at calibrating leaf positions across the entire range of leaf motion. There are only two parameters for calibrating leaf positions: a slope parameter (gain) and an intercept parameter (offset). Since there are many more possible leaf positions than there are variables, the linac cannot be calibrated to match the treatment planning system at all field positions. Instead, calibrating the MLC bank is limited to a “best fit,” where some individual leaf positions do not necessarily match the TPS calculations, but adjusting the MLC calibration further might make the overall fit worse.

Pinnacle^3 TPS, on the other hand, has a user editable offset table. At the time of linac commissioning, the default offset table was a light field offset table based purely on the geometry of how visible light would intercept the rounded leaf tip (Perrin & Neck, 2015). The TPS default values were not changed during machine commissioning. Since the offset table can have an entry for each leaf position, it has the capability to match the mechanical leaf positions throughout their entire range of motion, which would increase dosimetric accuracy of field edge position. Figure 1.6 schematically shows how leaf position is determined in the TPS and the linac.

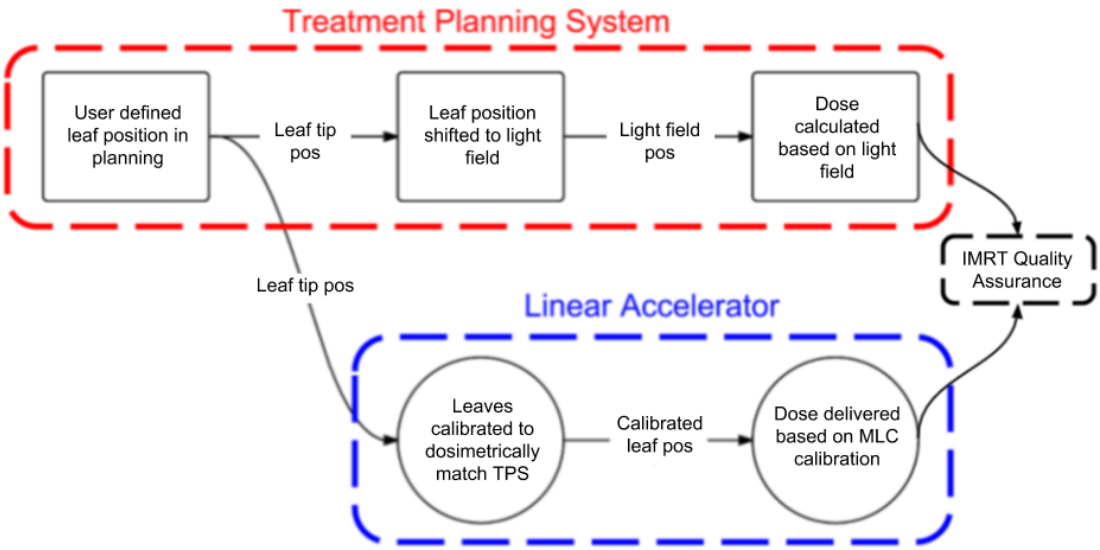

Figure 1.6: Flowchart showing how leaf position information flows between the TPS and the linac.

It was found that the TPS was significantly underestimating MLC transmission (see page 41 for more information). Additionally, the TPS has a tongue-and-groove width parameter, which governs the predicted interleaf leakage dose. Since the MLCi2 does not have a tongue-and-groove design, the tongue-and-groove width parameter was set to zero when the machine was originally commissioned (Perrin & Neck, 2015). While technically correct, this causes Pinnacle^3 to treat each MLC bank as if it were a solid slab, as if there was no interleaf gap at all. This contributes to the treatment planning system dose calculations underestimating the transmission through the MLC system.

1.4.2.Hypothesis

Improvement can be made to the accuracy of calculated 6 MV photon distributions using the Elekta MLCi2 system and the Phillips Pinnacle^3 commercial Treatment Planning System (TPS) by modifying the configuration

parameters of MLC transmission and leaf offset in the TPS. To test the hypothesis, we performed the following specific aims:

1.4.3.Specific Aim 1

Improve TPS dosimetric accuracy of 6 MV MLC shaped radiation fields by optimizing TPS parameters that govern MLC transmission and interleaf leakage.

1.4.4.Specific Aim 2

Improve TPS dosimetric accuracy of 6 MV MLC shaped radiation fields by optimizing parameters contained in the rounded leaf offset table.

1.4.5.Specific Aim 3

Compare dosimetric accuracy of calculated IMRT fields using original and improved TPS.

Chapter 2: Methods and Materials

2.1.Specific Aim 1: Measurement and Modeling of MLC Transmission

2.1.1.Measurement of MLC Transmission

Fields were planned in Philips Pinnacle^3 TPS to measure the transmission through the MLC. The jaws were set to form a 10x10 cm field (all jaws set to be retracted 5 cm from the central axis). Both banks of the MLC were set to be as far to the left as possible (13.5 cm and 12.5 cm to the left of the central axis), so that the 10x10 cm field formed by the jaws were completely covered by the right bank of the MLC.

Measurements of the 6 MV beam were made in solid water at a depth d_{max} (1.6 cm) with both ionization chambers and film. Ion chambers were placed at two locations within the 10x10 cm field: at isocenter and 0.5 cm lateral to isocenter. These two locations were used because an interleaf gap is located directly above isocenter, which will result in an increased apparent transmission, whereas 0.5 cm lateral to isocenter is located in the middle of the leaf where the dose contribution from interleaf leakage will be the smallest. The transmission through the MLC is equal to the ion chamber readings of the closed field relative to the readings from a field with the same jaw positions but with the MLC open (a standard 10x10 cm field). Two types of ion chambers were used; the Exradin Model A16 ion chamber (Standard Imagining Incorporated, Middleton, WI) and the PTW Model N300013 farmer type ion chamber (PTW Freiburg, Freiburg, Germany). These were chosen because of their very different sensitive volumes. The interleaf leakage radiation causes a complicated, non-uniform dose

distribution, and using multiple sizes of ion chambers allows us to take measurements with various amounts of dose averaging. See Table 2.1 for relevant ion chamber specifications.

Table 2.1: Ion chamber specifications. The CC13 is used in Section 2.2.1

Manufacturer:	Exradin	PTW	IBA Dosimetry
Model:	A16	N30013	CC13
Sensitive volume (cm^3):	0.007	0.6	0.13
Collector diameter (mm):	0.3	6.1	6.0
Collector length (mm):	1.27	23.6	5.8

2.1.2.Film Dosimetry

Carestream EDR2 radiographic film (Carestream Health Incorporated, Rochester, NY) was also used to measure the transmission through the MLC. The advantage of film is its very high spatial resolution, which is a benefit when measuring the complicated transmission patterns created by the interleaf leakage. 89 μm is the highest available resolution of the film scanner used, a Vidar Dosimetry Pro (Vidar Systems Corporation, Herndon, VA). The film's large size also makes it possible to measure the transmission through the MLC over the entire 10 cm x 10 cm field test field simultaneously, instead of measuring the transmission at a few individual points. Two film sizes were used: 25.4 cm x 30.5 cm and 35 cm x 43 cm.

However, film dosimetry presents additional challenges. Radiographic film has a complicated, non-linear dose response, which must be properly characterized. As the dose absorbed by the film increases, the sensitivity of the film drops until the film becomes saturated. An example sensitivity curve from RIT Classic Version 6.3 software (Radiological Imagining Technology Incorporated, Colorado Springs, CO) is shown in Figure 2.1.

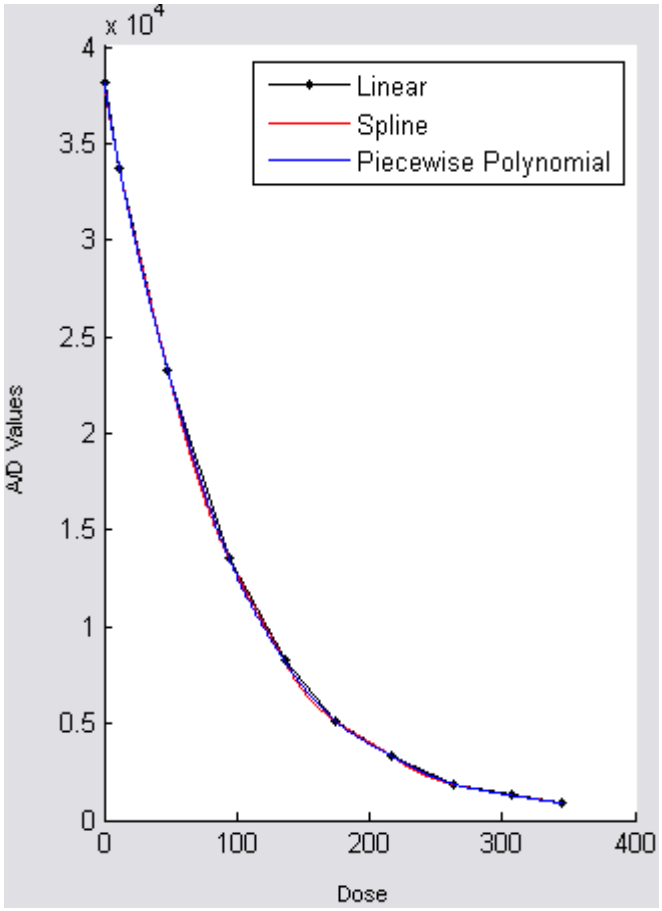

Figure 2.1: A screenshot RIT software showing a film calibration curve created for this work.

An 8-box calibration field was planned in order to measure the darkness of the film (i.e. the amount of transmitted visible light) of the film at various points throughout the film's sensitive range (0.1 to ~5 Gy). The field was designed to create two rows of four boxes, which were each 3x3 cm and spaced 4 cm apart. The boxes were shaped by the MLC and jaws. Each box received a different amount of Monitor Units (MU) such that the dose in each box varied in increments of roughly 50 cGy. The actual dose in each box of the calibration film was measured absolutely using a PTW N30013 ion chamber (see Table 2.1) in solid water at a depth of 10 cm with 10 cm of backscatter. These ion chamber measurements also recorded the scatter contribution from each open box to the

dose in every other box. Each session in which film measurements were made, this 8-box calibration field was also shot on film, which could then be used to create a sensitometric curve to calibrate the MLC transmission films (Figure 2.2).

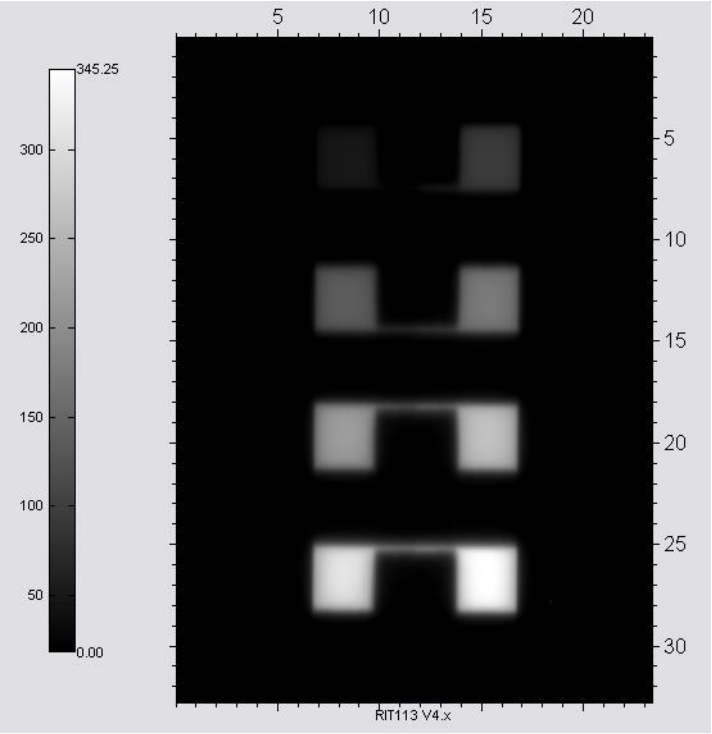

Figure 2.2: A screenshot of RIT software showing an 8-box calibration film. This film has been calibrated, so the brightness is proportional to dose delivered to the film. The dose is in units of cGy, while both the x and y axes are in units of cm.

Radiographic film must also be developed after being exposed to radiation, which presents additional challenges. The development process must be done in a dark room, as the films are sensitive to visible light and would be completely saturated if exposed to it. Film processing starts with the developer, which is a chemical bath consisting mainly of hydroquinone (Pai et al., 2007). The developer bath converts ionized silver bromide (AgBr) crystals in the latent image into metallic silver, which increases the optical density of the film (Pai et al., 2007). Once the film has been developed, the image is “fixed” in another

chemical bath which rinses off the un-ionized AgBr (Pai et al., 2007). Finally, the film is washed and dried to remove all chemicals from its surface except for the metallic silver which forms the desired image. We used a Konica Minolta SRX-101A film processor (Konica Minolta Incorporated, Tokyo, Japan), which moves the film through each of the chemical baths automatically.

The apparent optical density of the film is highly dependent on the activity of the various chemicals, which can change significantly with temperature (Pai et al., 2007). If multiple films are developed sequentially, the chemical baths will heat up from the machine's waste heat. In order to account for this effect, many old films, which had already been developed previously, were run through the processor continuously for about 10 minutes. At this point, it was assumed that the film processor had reached a temperature equilibrium, where the heat added from processing each film matched the heat dissipating from the processor unit. This was confirmed by developing multiple 8-box calibration films and verifying that the films gave consistent measurement results, indicating that the state of the processor did not change between films. Additionally, each of the chemical bath tanks were flushed and cleaned prior to film development, as chemical impurities can cloud the film and therefore the measured optical density.

For the picket fence tests used in this work, Gafchromic EBT3 radiochromic film (International Specialty Products, Wayne, NJ) was used for dose measurement instead of radiographic film. Initially radiographic film was used for the picket fence test, but it was found that this test produces a significant amount of scatter dose. Compton scattered photons will have significantly

reduced energy, and the response of radiographic film is highly dependent on photon energy. Radiographic film over-responds to low energy photons, so the picket fence test as measured by radiographic film reported a significantly higher dose. Radiochromic film response is effectively independent to photon energy at most diagnostic and therapeutic energies (keV and MeV photon energies) (Casanova Borca et al., 2012), and the picket fence test measurements performed very well.

There are several other significant advantages radiochromic film has over radiographic film. Due to its energy insensitivity EBT3 film is resistant to visible light and does not need to be kept in a light-tight envelope. This allows for easier handling than radiographic film, which must be kept in the dark at all times, and must be developed in a dark room. Furthermore, EBT3 film does not need to be developed at all, as the latent image will automatically begin to form in the 27 μm thick active layer, which contains the dyes and additives (Casanova Borca et al., 2012). Finally, the EBT3 film can be analyzed on three different color channels (RGB), which each has different characteristics and also allows for a much higher dose range than standard radiographic films (Pai et al., 2007). The red channel is most sensitive to doses below 8 Gy, the green channel is most sensitive to doses between 8 Gy and < 40 Gy, and the blue channel can be used for uniformity checks ("Gafchromic EBT3 Manual," 2011). For this work, the picket fence calibration film had a maximum dose of < 5 Gy, so only the red color channel was used for dosimetry.

It takes time for the chemical reactions to take place in the sensitive layer, but research shows that the net optical density will change less than 0.008 after two hours, and Casanova Borca et al. recommend waiting at least 30 minutes for low doses to allow the latent film image to stabilize (Casanova Borca et al., 2012). For this work, the radiochromic film was scanned 24 hours or more after exposure to ensure that the image was very stable.

The same 8-box calibration film and calibration protocol as described in Section 2.1.2 was used for both radiographic and radiochromic film. The radiochromic film was scanned using an Epson 10000XL flatbed color scanner (Seiko Epson Corporation, Nagano, Japan), and the calibration and analysis was performed with RIT software.

2.1.3.TPS Optimization

Once the transmission has been measured via film and ion chamber, these measurements can be used to optimize how the TPS calculates dose from transmission through the MLC. Specifically, there are three parameters governing these dose calculations: leaf transmission, tongue and groove width (in cm), and additional interleaf leakage transmission. The leaf transmission factor governs the transmission of x-rays through the entire thickness of a leaf and can be specified for various energies. The other two parameters govern the amount of radiation dose from x-rays that travel through the space between (Section 1.2).

2.1.4.Validation of MLC Configuration Parameters

Once the various MLC parameters were optimized we validated the TPSs dosimetric accuracy using the picket fence test. The design of the picket fence test consists of multiple 2.2 cm wide and 22 cm long subfields. The long edges of each subfield are defined by both leaf banks. The backup jaws were retracted 2 cm behind their respective leaf banks so that they didn't affect the shape of the open field. The 2.2 cm wide sides of the subfields abutted one another such that there was a 2 mm region of overlap between each subfield (Figure 2.3, Figure 2.4).

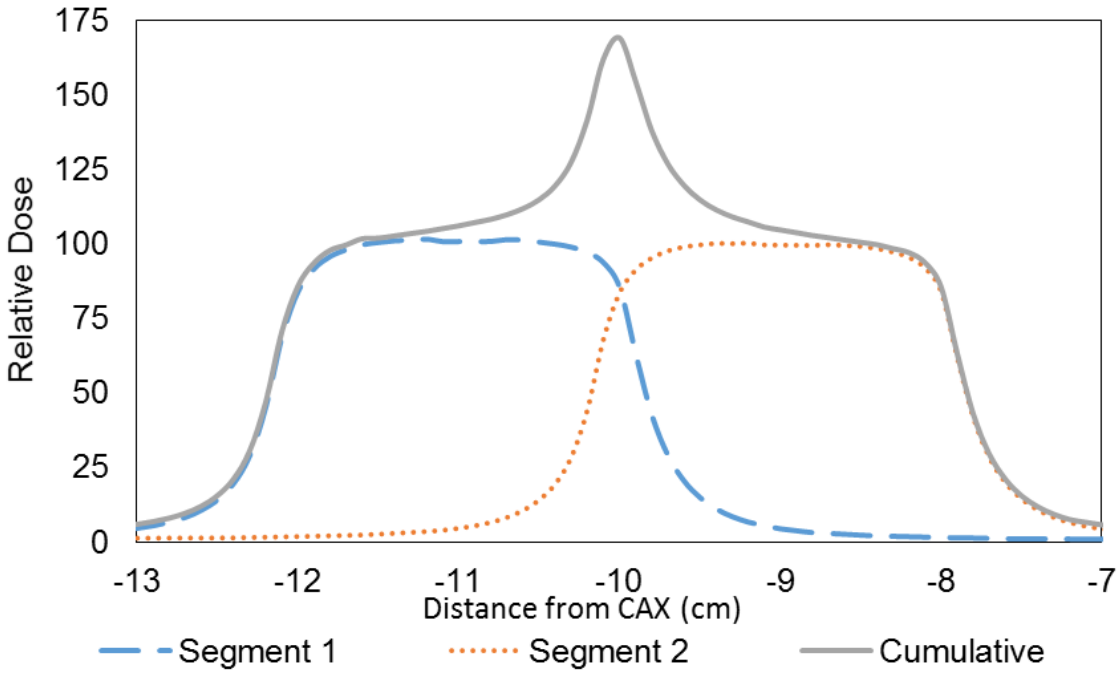

Figure 2.3: TPS calculated profiles showing two segments of a picket fence test and their cumulative dose.

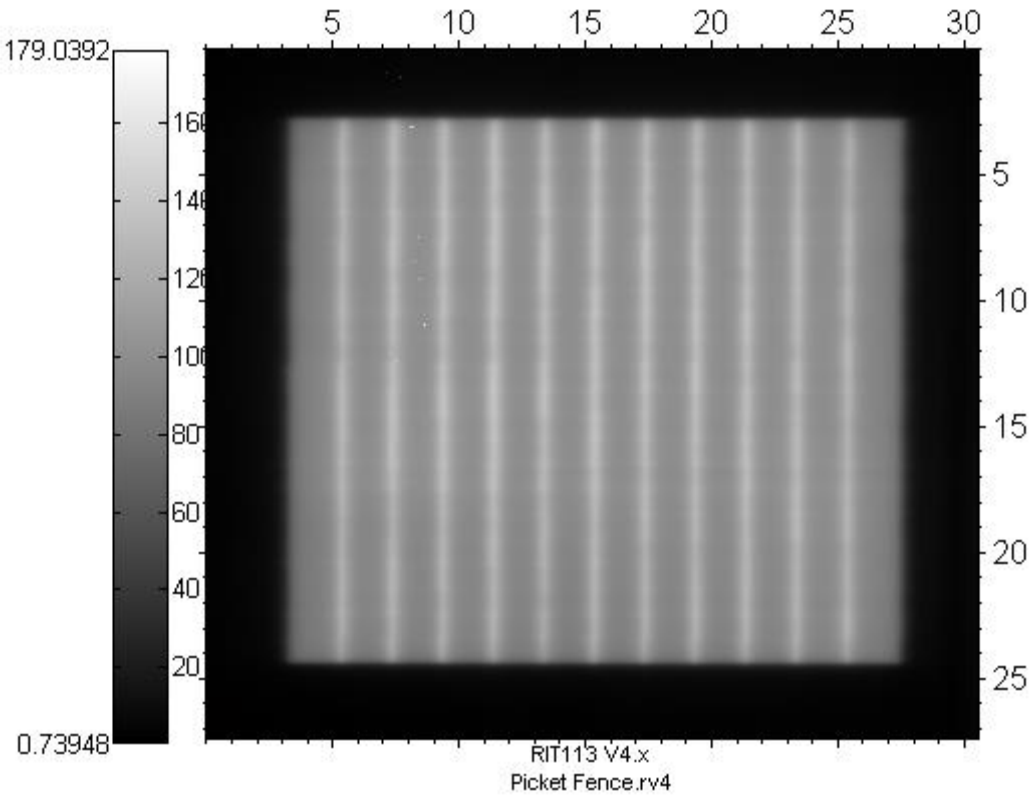

Figure 2.4: Picket fence test film. The bright vertical lines are regions of higher dose that result from overlapping segments.

Dose calculations for field abutment are sensitive to MLC transmission parameters because the dose distribution will be greatly affected by small changes to the location of the radiation field edge, which will in turn be affected by how radiation attenuation through the leaf tip is modeled. A similar picket fence type test was used by Williams and Metcalfe to validate improvements to the leaf transmission parameters of a Varian MLC system in the Philips Pinnacle^3 treatment planning system (Williams & Metcalfe, 2006).

The picket fence test was delivered with the linac and measured with film at a depth of 10 cm in solid water with 5 cm of backscatter. The picket fence test generates a significant amount of scattered x-rays, which are generally lower energy, causing radiographic film to over respond (Pai et al., 2007). Therefore

Gafchromic EBT3 film was used instead because its relative insensitivity to the energy spectrum of incident x-rays (Casanova Borca et al., 2012). Dose distributions for an identical situation were calculated with the TPS. Dose profiles between the film measurement and TPS calculations were compared to determine if the TPS calculation dosimetric accuracy had improved. Two comparisons were made: film measurement comparison to TPS calculation with default settings, and film measurement comparison to TPS calculation with optimized MLC transmission settings.

2.2.Specific Aim 2: Measurement and Modeling of Leaf Offset Table

2.2.1.Measurement of Rounded Leaf Offset

Fields were designed in the TPS to measure the location of the radiation field edge corresponding to leaf positions across the MLC's entire range of motion. Each field consisted of an 8 cm wide by 40 cm tall opening. The 40 cm long edges were defined by the MLC banks, with the backup jaws retracted 2 cm to ensure they would not encroach upon the open field (Rice, 2014). The first field was placed such that the left leaf bank was fully retracted (20 cm from the central axis), while the opposite leaf bank was fully extended (12 cm extended past the central axis) (Rice, 2014). This 8 cm wide field was delivered to a scanning water tank. A CC13 (Compact Chamber) ionization chamber (IBA Dosimetry GmbH, Schwarzenbruck, Germany) was attached to the tank's scanning apparatus and a profile was scanned across the 8 cm opening. The CC13 was chosen because of its relatively small sensitive volume (0.13 cm^3 vs 0.6 for the PTW N300013), which allows for greater spatial resolution. See Table

2.1 for more information. The ionization chamber's sensitive effective point of measurement was submerged to a depth of 2 cm in the water (Rice, 2014). The profile was scanned in the cross-plane direction, 0.5 cm lateral to the central axis. The profile was scanned at this location so that it was located directly underneath the center of a leaf, which reduced the dose contribution from interleaf leakage to a minimum. The scanned ionization profile had a spatial resolution of 0.6 mm. The dose was normalized to 100% at the center of the 8 cm wide by 40 cm wide field, which was usually not the maximum dose of the profile due to the dose horns present at a depth of 2 cm (Rice, 2014). An example profile is shown in Figure 2.5. Once the profile was normalized, the location of the radiation field edge, defined as the point in the penumbra where the radiation dose drops to 50% of the normalized value in the center of the open field, was located. Since the leaf offset is a function of leaf position, this procedure was repeated across the entire range of motion of the leaf bank in increments of 1 cm. This means that both leaf banks and both backup jaws were moved 1 cm to the right from their previous position and the profile rescanned to collect new data for those leaf positions. This field was repeated every 1 cm across the range of possible leaf positions, for a total of 33 profiles.

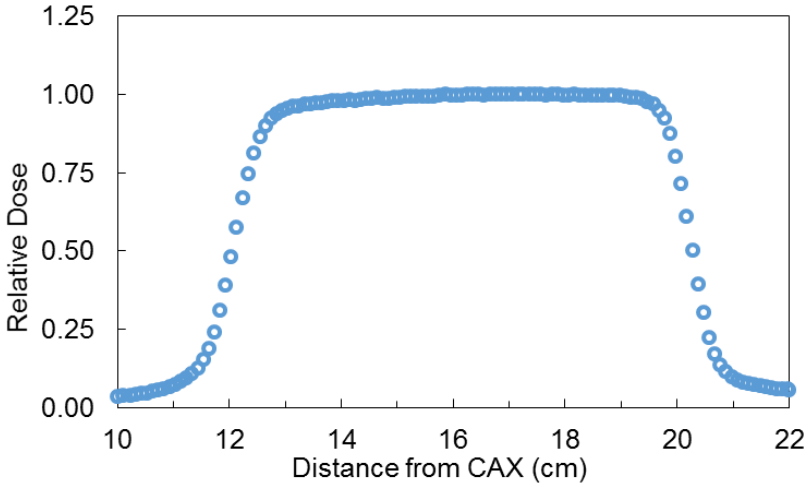

Figure 2.5: Sample dose profile scanned in water at a depth of 2 cm. Dose is normalized to the center of the 8 cm wide field. The edge of the radiation field (50% of the normalized dose) is determined from this data.

2.2.2.TPS Optimization

A machine with a zeroed out offset table (all table entries were zero) was created in the Pinnacle^3 treatment planning system. The 8 cm wide by 40 cm tall fields described in Section 2.2.1 were planned using the TPS with a zeroed out offset table. For each field, a planar dose was calculated at a depth of 2 cm in a water-box phantom. Profiles matching those described in Section 2.2.1 were extracted from the planar dose files. These profiles were also normalized to the center of the open 8 cm wide by 40 cm field and used to locate the position of the radiation field edge position (the point in the radiation penumbra where the dose drops to 50% of the dose at the center of the 8 cm wide field) which corresponded to the leaf bank positions of that field (Rice, 2014). These radiation field positions from the TPS dose profiles were compared to the radiation field positions measured from the water scanning tank profiles for each leaf bank position. The difference between the two is the rounded leaf offset for that

corresponding leaf position. A new machine was commissioned in the TPS with this “new” optimized offset table in place.

The position of the radiation field edge as calculated by the TPS is not only dependent on the leaf offset table, but also on the transmission factor of the MLC. Therefore, the leaf rounded offset optimization was done with the MLC transmission optimizations already applied, as described in Section 2.1.

2.2.3.Validation of New Offset Table

The picket fence test, as described in Section 2.1.4, is also a suitable method to test changes to rounded leaf offset table (Rice, 2014). This is because the size of the region of overlap between abutted fields is very sensitive to leaf bank position. Small changes in the TPS’s leaf offset table can significantly affect the shape and magnitude of the dose profile calculated by the TPS.

To validate the optimizations to the rounded leaf offset table, dose profiles were calculated with the two different cases in the TPS: with the default offset table applied and with the “new” table.

2.3.Specific Aim 3: Evaluation of IMRT Performance

2.3.1.Selection of IMRT Plans

In order to test how the modifications to the TPS parameters affected calculations of delivered dose distributions, 19 conventional, gantry-static IMRT fields from three different patients’ treatment plans were selected. Gantry-static fields were chosen because they could be delivered orthogonally into the measurement plane. The specific fields used were chosen simply because they were recently delivered gantry-static plans. 10 of the fields came from two breast

cancer patients, and were treated with similar plans. Most of the treatment dose for these patients came from parallel-opposed, tangent, non-IMRT fields. Each patient was also treated with five different gantry-static IMRT fields to better shape the dose in the breast. We analyzed each of the five IMRT fields from both patients. These fields usually had a relatively low dose, so the fields' MUs were increased to put the maximum dose in the middle of radiographic film's sensitive range (~2.5 Gy).

The remaining nine fields that were analyzed were developed specially for this project. We wanted to analyze a Stereotactic Body Radiotherapy (SBRT) plan because they usually consist of high doses delivered by very small fields, so errors in leaf position will be larger relative to the size of the treatment field. However, MBPCC does not treat SBRT cases with gantry-static IMRT, so a clinically realistic plan was developed. A lung cancer patient was selected and nine SBRT gantry-static IMRT fields were planned at gantry angles every 40° around the patient. These nine fields were planned under the guidance of MBPCC dosimetry staff to ensure that the SBRT fields were clinically realistic.

Planar dose measurements of these plans were captured using two different measurement approaches: radiographic EDR2 film and the MapCHECK2 (Sun Nuclear Corporation, Melbourne, FL), a 2-D array of diode detectors. The MapCHECK2 is a tool specifically designed for IMRT QA. It consists of a planar array of 1527 diode detectors with a uniform 7.07 mm spacing ("MapCHECK 2 Manual," 2015). Its maximum measurable field size is 32 cm wide by 26 cm tall ("MapCHECK 2 Manual," 2015), which is smaller than

the maximum available film size (43 cm x 35 cm), but is still more than adequate to make planar dose measurements. See Section 2.3.2 for a discussion about dosimetry with film and the MapCHECK2. Film was placed in the isocentric plane under 5 cm of solid water buildup with 5 cm of solid water backscatter. The MapCHECK2 measurements were done with the device placed in a rectangular water equivalent plastic phantom called the MapPHAN. The MapPHAN was placed at 95 cm SSD. The MapPHAN depth is radiologically equivalent to 5 cm of water but the physical depth is only 4.1 cm, which results in the measurement plane being located at 99.1 cm from the source, which is 9 mm above the isocentric plane. Although these 19 plans would be delivered clinically at a variety of different gantry angles, we wanted to make planar dose measurements with the measurement plane orthogonal to the collimator, so all gantry angles were set to 0° (so that the collimator is pointed straight down onto the treatment couch) (Figure 2.6).

Planar dose files were generated which exactly matched measurement conditions. Film dose calculations were done with a CT image set of a rectangular water equivalent plastic phantom, and the MapCHECK2 dose calculations were done with a CT image set of the MapCHECK2 inside its water equivalent plastic phantom. These TPS planar dose calculations were compared to their respective planar dose measurements. Agreement between dose calculations and dose measurements was evaluated using gamma index analysis. See Section 2.3.3 for a discussion of gamma index analysis. A total of four gamma index analysis cases were performed: measurement to default TPS

calculation, measurement to TPS calculation with optimized MLC transmission, measurement to TPS calculation with optimized rounded leaf offset table, and measurement to TPS calculation with both optimized MLC transmission and optimized rounded leaf offset table. An inter-comparison between the gamma index passing rates of these various cases will quantify the difference in dosimetric performance after TPS configuration changes described by Aims 1 & 2 have been made.

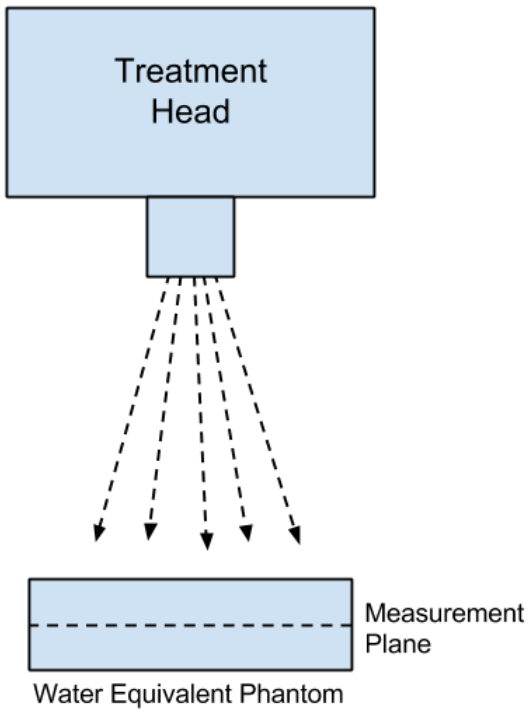

Figure 2.6: Diagram showing general IMRT measurement setup. All IMRT plans were delivered to an orthogonal measurement plane inside a water equivalent plastic phantom.

2.3.2.MapCHECK2 Dosimetry

The MapCHECK2 is advantageous because it can make quick absolute dose measurements, and is relatively insensitive to photon energy and dose rate effects. It is simple to use, as it only requires one data/power cable, and dose

measurements can be made after a quick background radiation check and a quick output calibration. Output is checked by delivering 100 MU of a standard 10 cm x 10 cm field, and telling the software what the known dose value at the center of the field (92.9 cGy). SNC Patient Ver. 6.2.2 (Sun Nuclear Corporation, Melbourne, FL) software was used to record and analyze data. The planar dose data is available for analysis immediately after measurement takes place, an advantage over radiographic film, which must be left to sit for at least an hour after dose delivery, must be processed in a dark room, and must be calibrated to be used for absolute dosimetry (Pai et al., 2007). However, the disadvantage of the MapCHECK2 is that it has relatively poor spatial resolution (7.02 mm uniform spacing between diodes) relative to that of film (up to 89 microns).

Planar diode arrays are used for patient-specific QA of IMRT plans at many clinics. By using the planar diode array for Aim 3 of this project, we used clinical QA measurement methods. Measuring the same fields with radiographic film does not replicate clinical practice because it is generally not used for QA. However, because the film has superior spatial resolution, it will provide us with more information about the agreement between actual planar dose distributions and dose calculations by the TPS.

2.3.3.Gamma Index Analysis

Gamma index analysis is a test that quantifies agreement between two data sets. It was originally proposed by Low et al. in 1998 for the specific purpose of quantifying the agreement between the measured and TPS calculated dose of a radiotherapy plan. Gamma index analysis uses two criteria to evaluate

agreement: percent dose difference (ΔD_M), and distance-to-agreement (DTA or Δd_M) (Low et al., 1998). Percent dose difference is used to compare the dose of the target calculated point relative to the dose of a reference measured point. DTA is used as a criteria to help evaluate high dose gradient regions, as a small setup or positional error could cause a very large percent dose difference in a high gradient region, even if a point with the correct dose was located very nearby. This point could fail a percent dose difference check, but still pass a DTA check. Gamma index analysis looks at both criteria simultaneously.

Gamma index values are calculated between the reference point in the measured dose plane, and the comparison point in the calculated dose plane, or

$$\Gamma(\boldsymbol{r_m}, \boldsymbol{r_c}) = \sqrt{\frac{(\boldsymbol{r_c} - \boldsymbol{r_m})^2}{\Delta d_M^2} + \frac{\delta^2(\boldsymbol{r_m}, \boldsymbol{r_c})}{\Delta D_M^2}} \qquad 2.1$$

where $\mathbf{r_c}$ and $\mathbf{r_m}$ are respectively the locations of the calculated and measured dose points being considered, and $\delta(\mathbf{r_c}, \mathbf{r_m})$ is the percent dose difference between the calculated and measured dose points being considered (Low et al., 1998).

Equation 2.1 is essentially the formula for a three dimensional ellipsoid in dose space, centered at the reference point being considered in the measured dose plane (Low et al., 1998). Two of the radii of the ellipsoid are equal to the DTA criteria (Δd_M), while the third radius is equal to the percent dose difference criteria (ΔD_M) (Low et al., 1998). If any point in the calculated dose plane falls within the surface of the ellipsoid, it has a gamma value of less than one, and the reference point is considered “passing” (Low et al., 1998)

$$\gamma(\boldsymbol{r_m}) = \min\{\Gamma(\boldsymbol{r_m}, \boldsymbol{r_c})\}\,\forall\{\boldsymbol{r_c}\} \qquad 2.2$$

Equation 2.2 simply states that each individual point in the measured reference dose plane is compared to every single point in the calculated dose plane, and the minimum gamma comparison value is taken as the γ value for that point. Again, γ ≤ 1 means that the associated reference point is considered to pass the criteria, while γ > 1 means that the associated reference point has failed the criteria and does not conform to the calculated dose.

According to MBPCC policies and procedures, patients may be treated as long as 90% of the reference points pass with γ ≤ 1 with criteria ΔD_M = 3 % and Δd_M = 3 mm (Perrin & Neck, 2015) (Ezzell et al., 2003). In practice, the more stringent criteria are almost always used, and a plan that had less than 95% pass rate with the more stringent criteria would usually be re-planned or rechecked to make sure a mistake had not been made. The majority of IMRT plans at MBPCC pass the more stringent criteria.

2.3.4.Additional Work

In order to explore other effects that influence IMRT QA results in this work, the beam was remodeled in Philips Pinnacle^3 to demonstrate that other parameters are more responsible for the quality of the treatment planning system calculations at the depth that planar doses were measured (5 cm). New parameters were chosen specifically to improve the accuracy of the TPS model at a depth of 5 cm in water, relative to the commissioning data.

First, a change was made to a parameter governing how scatter from the flattening filter is modeled. The model of scatter from the flattening filter has a

significant impact in the tail region of a dose distribution. The TPS models this scatter with a Gaussian function. The user is able to modify both the width and the magnitude of the Gaussian function. For this additional investigation, the magnitude of the Gaussian was changed from a default value of 0.08238 to 0.057 and the width of the Gaussian was changed from 1.48136 to 1.2. These changes significantly reduced the total amount dose in the tail regions.

Second, a parameter governing the source size was changed. The source size perpendicular to the gantry axis was reduced from 0.1828 cm to 0.1785 cm. The source size has a strong effect on the shape and width of the penumbra. Reducing the source size reduced the width of the geometric penumbra.

Finally, small changes were made to parameters governing the amount of fluence through the flattening filter. These changes are shown in Figure 2.7 and Table 2.2. These TPS parameters control the energy fluence through the flattening filter as a function of distance from the center of the flattening filter. Generally, the fluence would be expected to increase linearly with radius. Only the energy fluence values at the lowest radii (≤ 3.53553 cm) were remodeled. Energy fluence values at larger radii (up to 28.2843 cm) were not remodeled. Changing these parameters increased the quality of fit in the open field region. The complete default and remodeled energy fluence values as a function of radius can be found in Figure 2.7.

While altering these parameters, dose profiles were recalculated and compared to the original measured data used to commission the machine, which includes many profiles of various square and rectangular fields at a variety of

depths. Since IMRT QA is always done at a depth of 5 cm, the various model parameters were altered while only trying to optimize the agreement between the TPS calculations and commissioning data at a depth of 5 cm. The remodeling of the parameters described above was not based on physics or direct measurements. Rather they were only changed with the objective of improving the TPS calculation accuracy relative to the original measured commissioning data.

The optimized leaf transmission factor of 0.005 and the optimized rounded leaf offset table were also included in this remodel. After all of the changes were made, this new beam was used to recalculate the IMRT and picket fence test planar dose distributions for all fields.

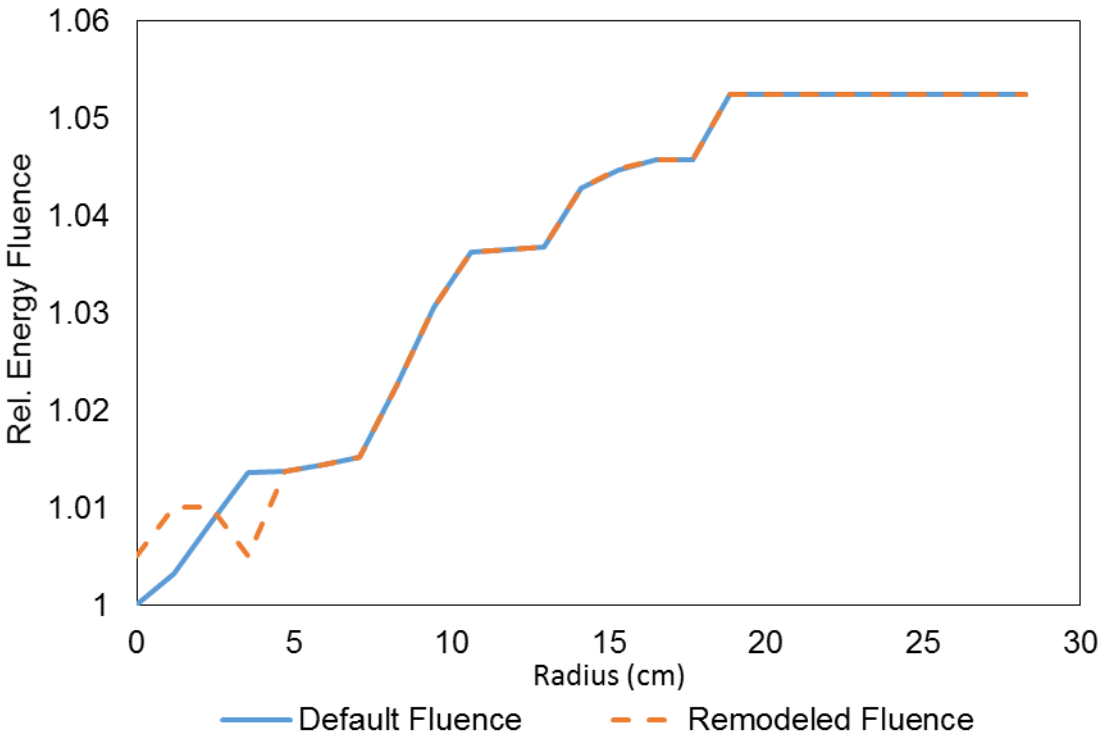

Figure 2.7: Complete flattening filter energy fluence values.

Table 2.2: Changes made to the flattening filter energy fluence at the specified radii.

Radius (cm)	Default Fluence	Remodeled Fluence
0	1	1.005
1.17851	1.00321	1.01
2.35702	1.00851	1.01
3.53553	1.01367	1.005

Chapter 3: Results

3.1.Aim 1 Results

3.1.1.MLC Transmission and Leakage

Figure 3.1 shows a comparison between film measurement and TPS calculations of dose leaking through the MLC at a depth of 2 cm in water equivalent plastic. The field was formed with a 10 cm wide by 20 cm tall jaw opening, with the right leaf bank positioned at -12.5 cm, completely covering the opening in the jaws. The TPS dose calculation significantly underestimated the transmission through the MLC. The film profile shows significant peaks resulting from interleaf leakage, as well as smaller peaks between the interleaf leakage peaks. The structure of this profile is discussed further in Section 4.1.

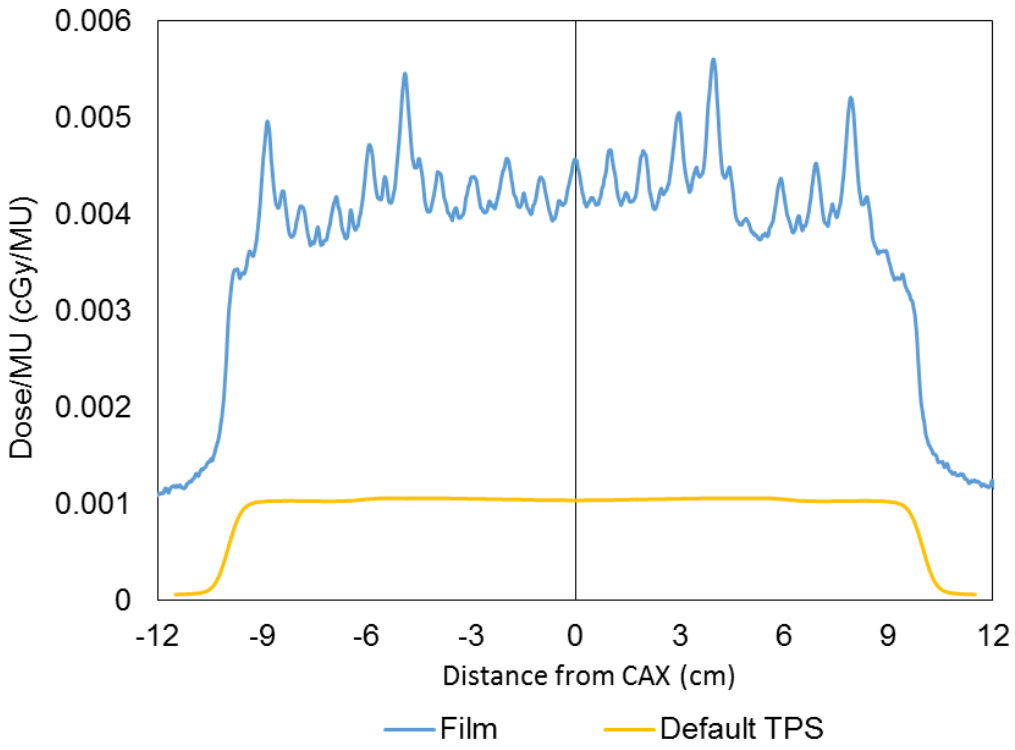

Figure 3.1: Film and TPS profiles of MLC transmission.

3.1.2.Measurement of MLC Transmission

Figure 3.2 shows a comparison between radiographic film and ion chamber measurements of the transmission through the MLC. These measurements were made with a 10 cm by 10 cm opening in the jaw. The transmission is defined as the dose with the MLC bank closed over the jaw opening relative to the dose measured with the jaws retracted. The measurements were taken at a depth of d_{max} (1.6 cm) in water equivalent plastic. Table 3.1 contains the ion chamber measurement data.

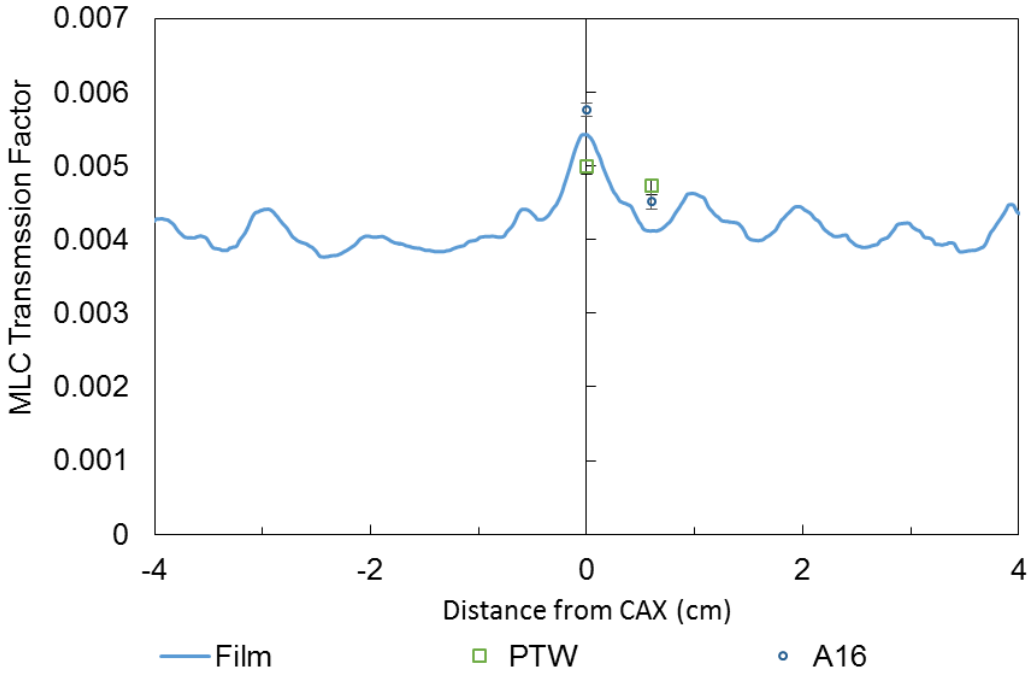

Figure 3.2: MLC transmission as measured by film and ion chambers.

Table 3.1: Ion chamber measurements of transmission. This data is shown graphically in Figure 3.2.

Chamber type	Chamber Position	Measured Transmission
Exradin A16	isocenter	0.00576093
Exradin A16	y=0.5 cm	0.00452188
PTW N30013	isocenter	0.00499183
PTW N30013	y=0.5 cm	0.00472904

The film measurements show a slightly lower MLC transmission value than measurements with ion chambers. This may be because radiographic film is highly sensitive to film energy. When the x-rays from the source are filtered through the MLC, lower energy x-rays are preferentially attenuated, resulting in a significantly higher average photon energy. The EDR2 film under-responds to higher energy spectrum, resulting in a lower transmission result.

For this reason, the ion chamber measurements were used for the final MLC transmission value. Ion chambers were placed at two locations: isocenter and 0.5 cm lateral to isocenter. Ultimately, the average of all ion chamber measurements was used as the leaf transmission value: 0.005. This is five times higher than the leaf transmission value in the currently used clinical machine of 0.001. This essentially represents an average transmission value in the peaks and valleys of the measured transmission profile.

3.1.3.Picket Fence test

Figure 3.3 shows the picket fence test results. A radiochromic film profile measurement is compared to the default TPS and transmission-optimized TPS dose profile calculation. Significant improvement is seen when the TPS leaf transmission is set to 0.005 instead of 0.001. One metric to quantify the performance of a picket fence test is the peak-to-valley ratio (Williams & Metcalfe, 2006). The mean peak-to-valley ratio is the ratio of the dose in the overlap region relative to the dose in its two adjacent valleys (Williams & Metcalfe, 2006). The film measurement had a mean peak-to-valley ratio of 1.25 ± 0.02, while the default TPS calculation had a ratio of 1.196 ± 0.006. Optimizing

the leaf transmission factor resulted in a mean peak-to-valley ratio of 1.205 ± 0.003, closer to the measured film ratio, which indicates that optimizing the leaf transmission factor improves TPS accuracy.

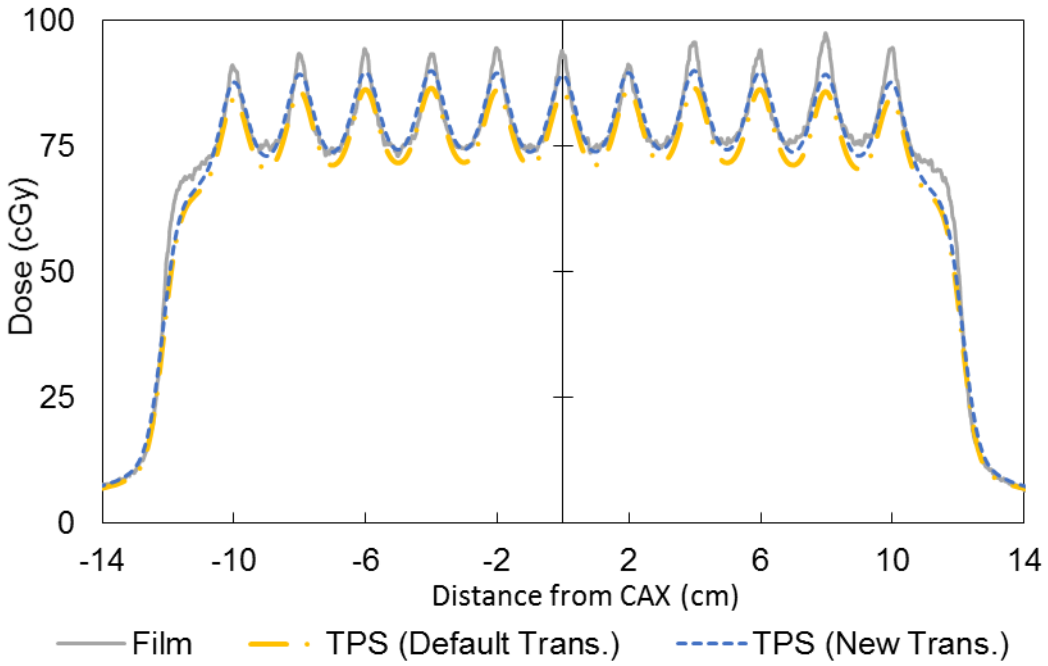

Figure 3.3: Picket fence test comparison using default TPS setting and optimized transmission parameter.

3.2.Aim 2 Results

Figure 3.4 shows one of the 8 cm wide field profiles measured with the CC-13 ionization chamber and the complimentary TPS calculated dose. In this figure, the left leaf bank was positioned at -12 cm and the right leaf bank was positioned at 20 cm.

Table 3.2 lists the field edge positions and optimized offset values from all these profiles. These field edge positions (both measured and TPS calculated) were found for both left and right leaf banks at each position. The values were averaged across both leaf banks. The optimized offset table is graphed and compared to the default offset table in Figure 3.5.

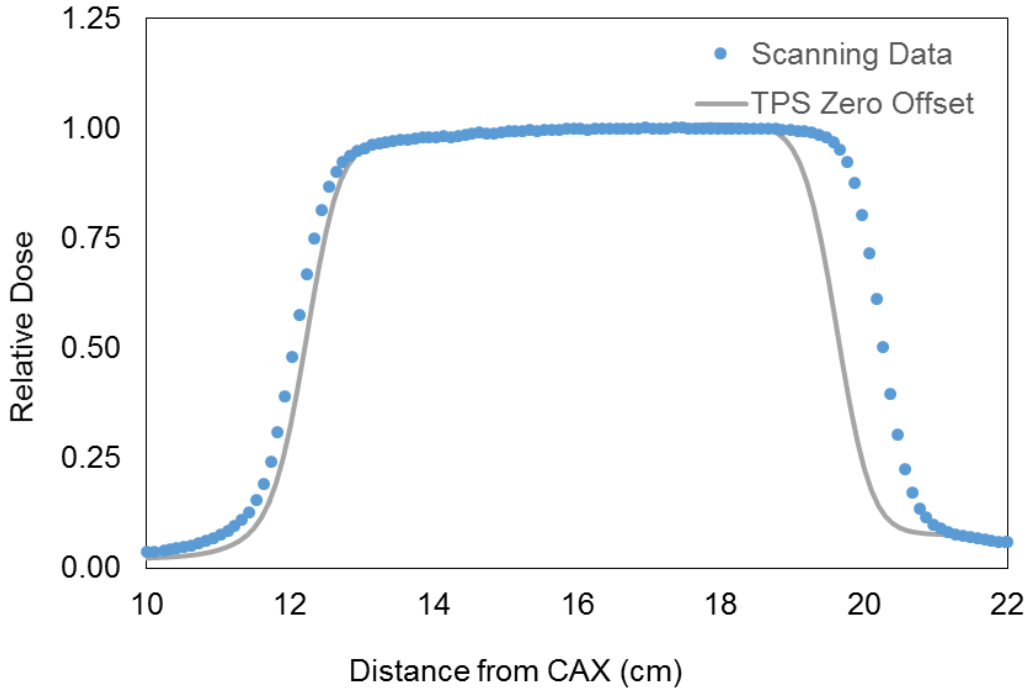

Figure 3.4: Normalized calculated and scanned profiles for an 8 cm wide field. The left leaf bank was positions at -12 cm and the right leaf bank was positioned at 20 cm.

A new machine was commissioned with the optimized offset table and the profiles were recalculated. A sample profile is shown in Figure 3.6. For this sample profile, the user defined leaf position for the right leaf bank was 14 cm. The actual measured leaf bank position was 14.17 cm. The TPS calculated field edge position with the default offset table is 14.09 cm, while the TPS calculated field edge with the optimized offset table is 14.18 cm, significantly closer to the measured radiation field edge location.

Table 3.2: Field edge positions and optimized leaf offset values. The field edge positions represent the distance from the central axis. The offset table is simply the difference between the calculated and measured field positions. This data is displayed graphically in Figure 3.5.

User Defined Position (cm)	Measured Field Edge (cm)	Calculated Field Edge (cm)	Optimized Offset (cm)
20	20.288	19.672	-0.616
19	19.304	18.686	-0.619
18	18.284	17.690	-0.594
17	17.274	16.698	-0.576
16	16.231	15.703	-0.527
15	15.207	14.704	-0.503
14	14.192	13.709	-0.483
13	13.196	12.766	-0.429
12	12.157	11.819	-0.337
11	11.164	10.872	-0.292
10	10.144	9.918	-0.226
9	9.127	8.946	-0.181
8	8.134	8.002	-0.131
7	7.130	7.008	-0.122
6	6.126	6.039	-0.087
5	5.110	5.073	-0.037
4	4.109	4.105	-0.005
3	3.092	3.104	0.013
2	2.078	2.104	0.025
1	1.070	1.108	0.038
0	0.069	0.096	0.027
-1	-0.934	-0.908	0.026
-2	-1.951	-1.911	0.040
-3	-2.949	-2.915	0.035
-4	-3.955	-3.923	0.031
-5	-4.983	-4.962	0.022
-6	-5.985	-5.996	-0.010
-7	-6.991	-7.016	-0.025
-8	-7.997	-8.026	-0.029
-9	-8.984	-9.090	-0.106
-10	-9.990	-10.113	-0.122
-11	-11.015	-11.181	-0.166
-12	-12.057	-12.211	-0.154

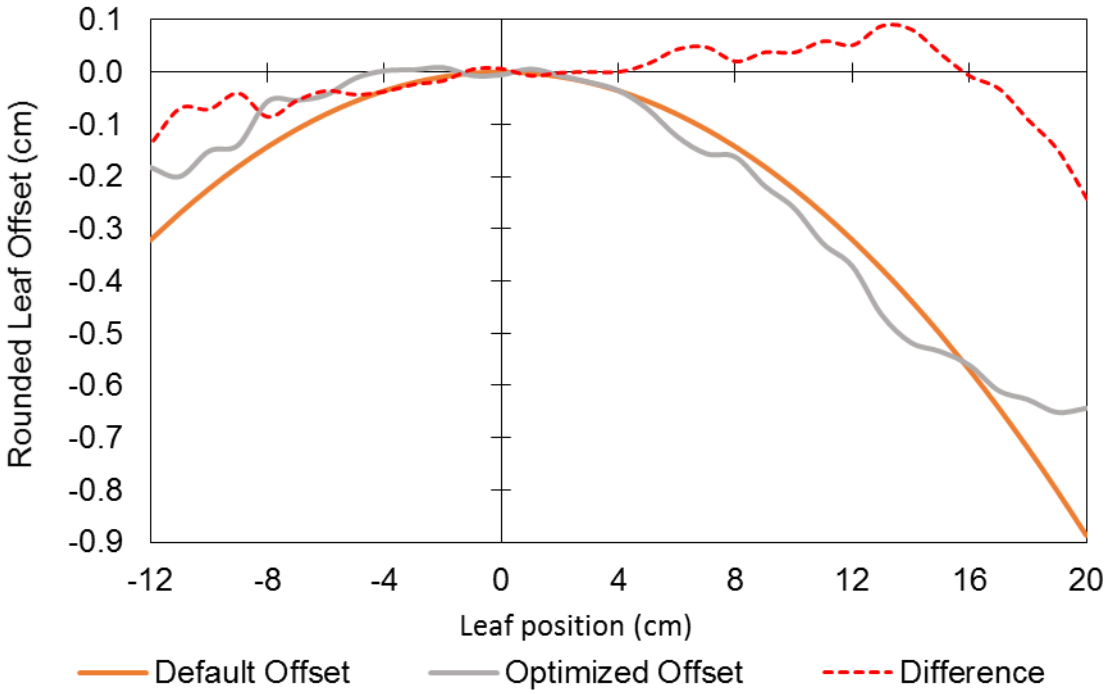

Figure 3.5: Comparison between default and optimized offset tables.

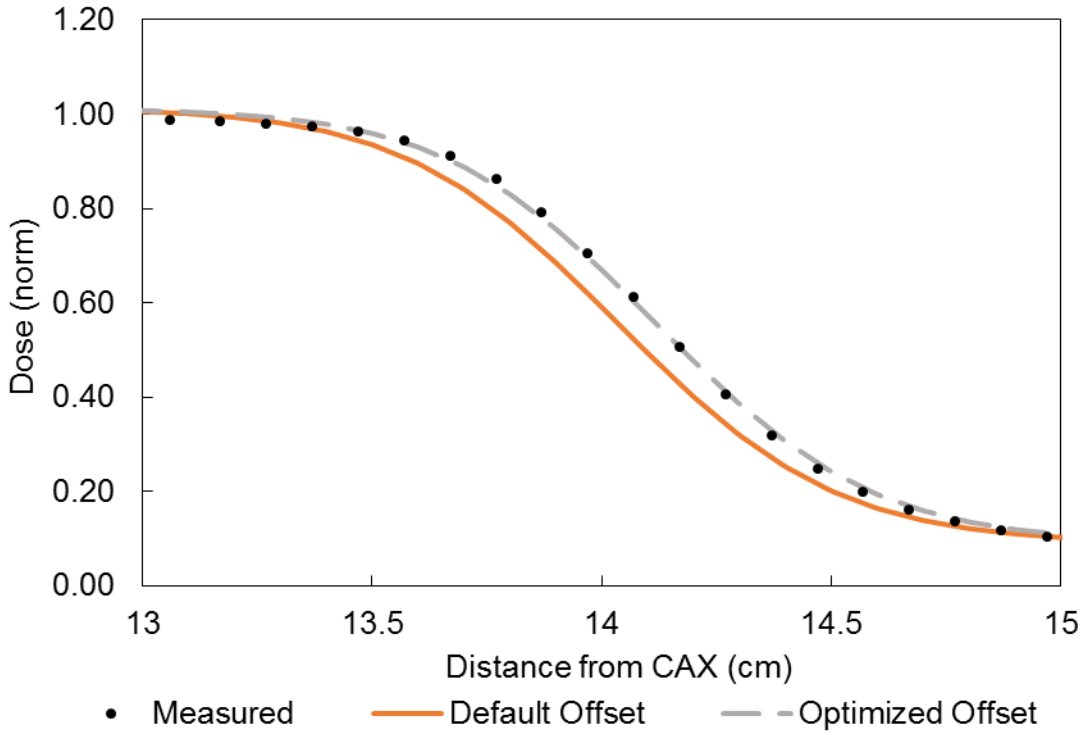

Figure 3.6: A sample penumbra comparison between measured data, TPS calculations with default offset table, and TPS calculations with optimized offset table. The right leaf bank is positioned at 14 cm (i.e. extended past the central axis).

3.2.1.Picket Fence Test

Figure 3.7 plots picket fence test results from measurement, TPS calculations with default and optimized offset table. The results reveal little change in the TPS accuracy. After optimizing the leaf offset table values, the mean peak-to-value ratio was 1.20 ± 0.02, no significant difference from the default TPS case. The overlap regions centered at ± 6 cm from the central axis shows a slight improvement, while the overlap regions centered at ± 8 cm from the central axis shows a slight worsening of performance.

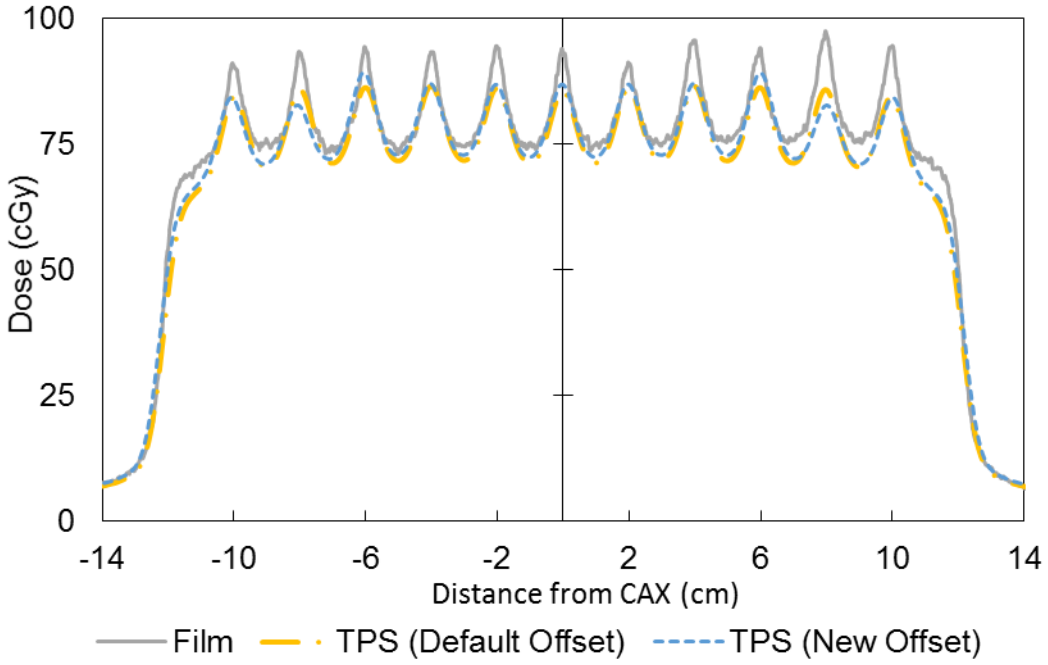

Figure 3.7: Picket Fence test comparison with only offset table optimized.

Figure 3.8 plots the picket fence test results from the radiochromic measurements to the default TPS dos profile and TPS profile with both optimized leaf transmission parameters and offset table values. The optimized TPS calculation shows a small improvement in the overlap region close to the central axis, and a significant improvement in the valley regions at all leaf positions.

However, the TPS calculation with optimized leaf transmission and optimized rounded leaf offset table performs significantly worse than the TPS calculation with only leaf transmission optimized. This result is discussed further in Section 4.2. Overall, the mean peak-to-valley ratio dropped to 1.17 ± 0.02, a worsening of performance relative to the default TPS case.

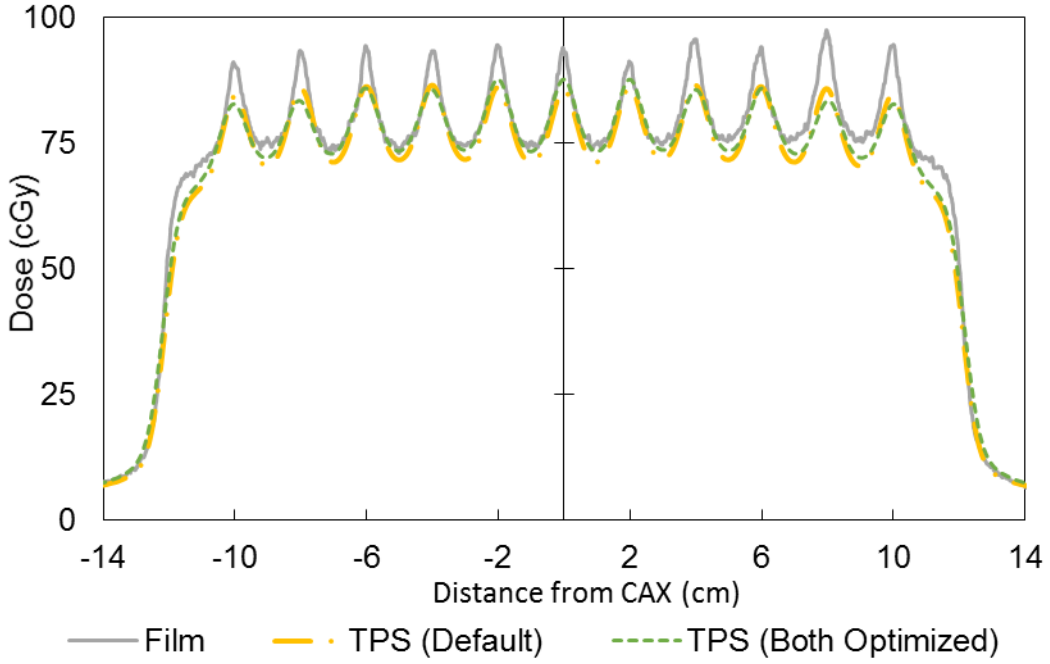

Figure 3.8: Picket Fence test comparison with both transmission and offset optimized.

3.3.Aim 3 Results

3.3.1.Planar Diode Array Results

Figure 3.9 shows a representative IMRT plan measured with the planar diode array. The gray shading represents the dose distribution as calculated with default parameters in TPS. The red and blue dots represent planar diode array measurements that do not match within the applied Gamma index criteria. Red dots represent diode measurements that recorded higher dose than the TPS dose calculation at that position, and blue dots represent diode measurements

that recorded lower dose than the TPS dose calculation at that position. A stringent criteria of ΔD_M = 1 % and Δd_M = 1 mm was used for this illustrative example of how the agreement of measured and calculated dose distributions was visualized. In general, the TPS default dose distribution is lower in the open field region and too high in the out-of-field regions.

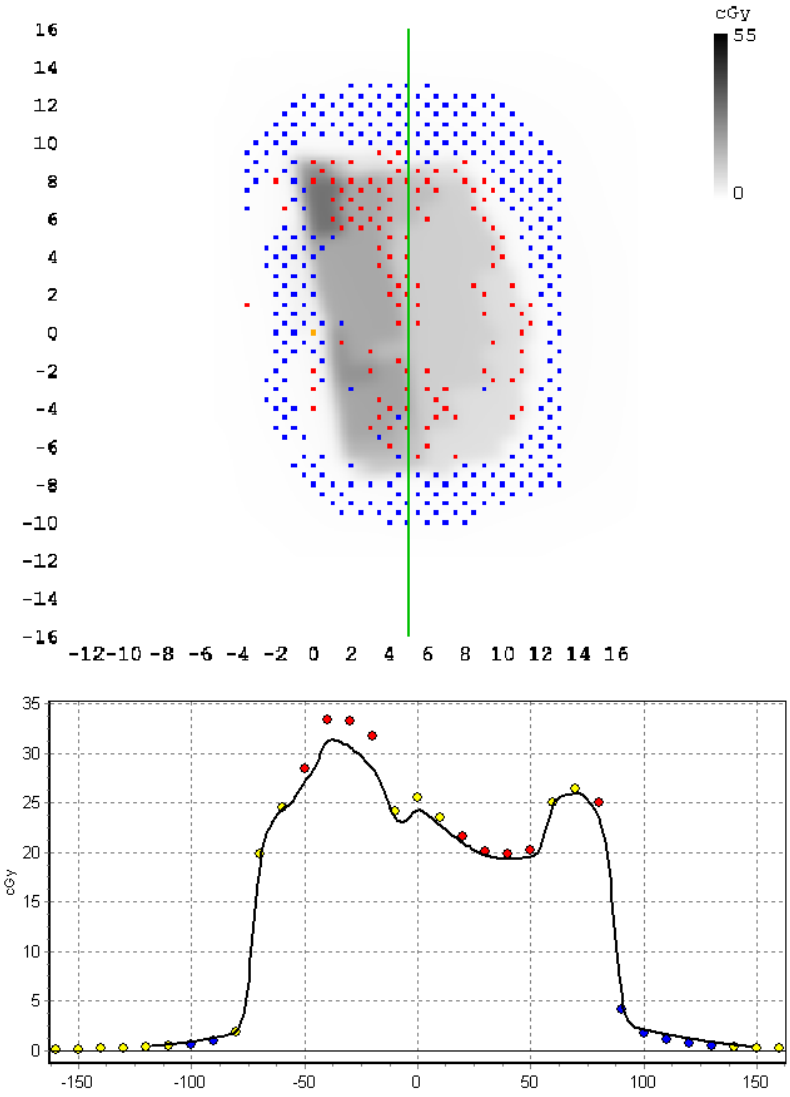

Figure 3.9: Field 1 measured with planar diode array and compared to default TPS calculation. The green line represents the profile seen in the bottom of the figure. Blue dots represent diode dose measurements that are lower than the TPS calculation, red dots represent measurements that are higher. The solid line represents TPS calculation. All dimensions in cm.

Figure 3.10 shows gamma index analysis between the planar diode array measurement and default TPS calculation using clinical gamma criteria (ΔD_M = 3 %, Δd_M = 3 mm) of Field 1. This comparison has a passing rate of 98.1%. Optimizing only the transmission parameter results in a passing rate of 97.5%, as shown in Figure 3.11. Optimizing both the transmission and the offset table resulted in a passing rate of 96.7%, as shown in Figure 3.12. The results of Field 1 are generally representative of the planar diode array analysis as a whole.

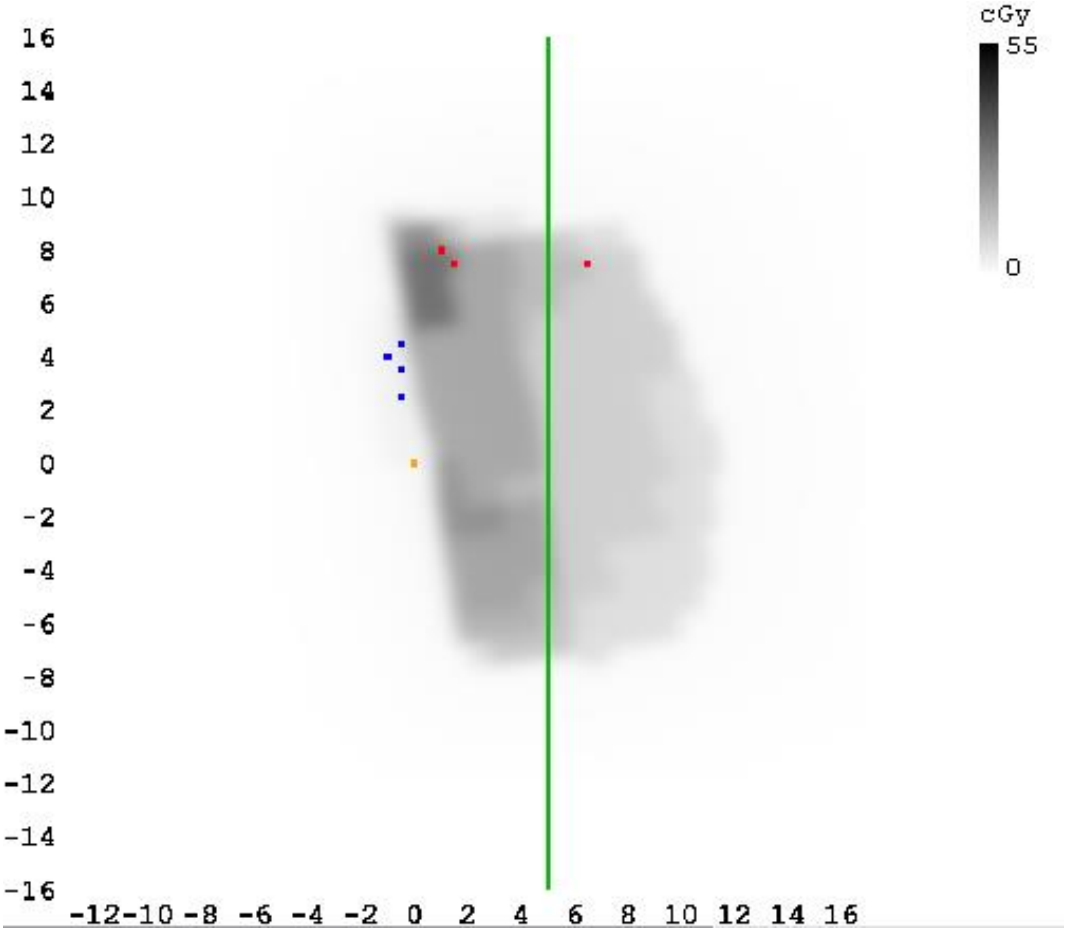

Figure 3.10: Field 1 gamma comparison between planar diode array measurement and default TPS calculation using clinical gamma index criteria. Dimensions in cm. Passing rate: 98.1%

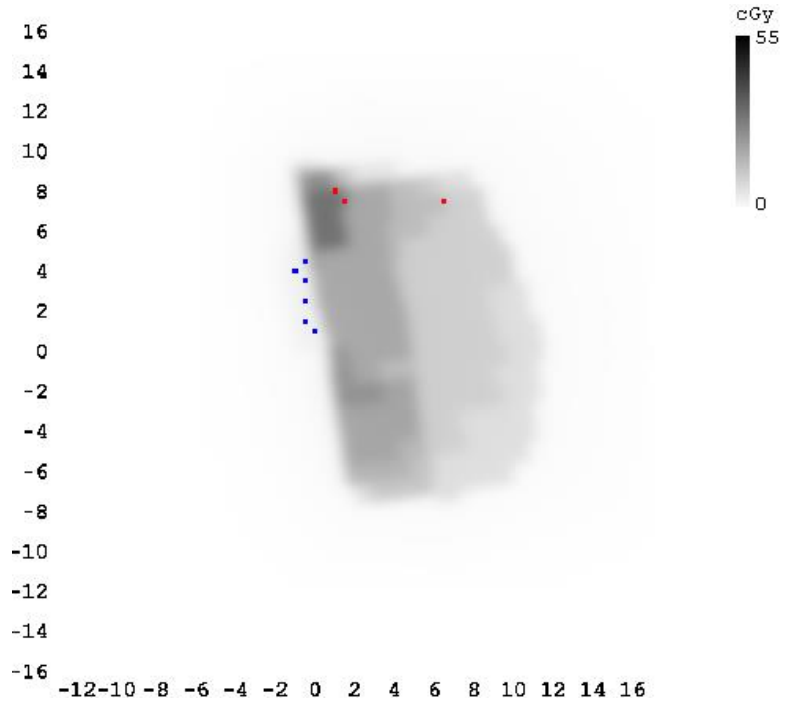

Figure 3.11: Field 1 gamma comparison between planar diode array measurement and TPS calculation with optimized MLC transmission using clinical gamma index criteria. Dimensions in cm. Passing rate: 97.5%

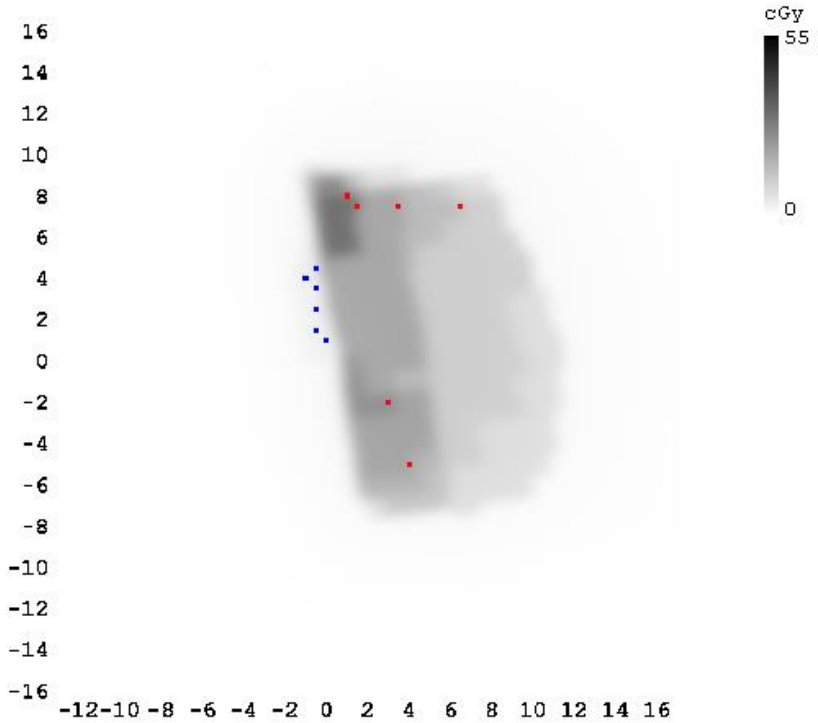

Figure 3.12: Field 1 gamma comparison between planar diode array measurement and TPS calculation with optimized MLC transmission and optimized offset table using clinical gamma criteria. Passing rate: 96.7%

Table 3.3 contains all gamma index results for planar diode array measurements. Optimizing only the leaf transmission factor results in an average -1.48 ± 2.1 % change in gamma index passing rate. Using a paired Student's t test and the Wilcoxon Signed Rank test, p-values were calculated to be 0.00630 and 0.00188 respectively, showing that planar diode IMRT QA passing rates worsened significantly after optimization of leaf transmission at a significance level of $p = 0.05$.

Optimizing only the leaf offset table results in an average 0.01 ± 0.2 % improvement in gamma index passing rate. A paired Student's t test p-value was calculated to be 0.87318, showing that planar diode IMRT QA passing rates were not significantly different at a significance level of $p = 0.05$. The Wilcoxon Signed Rank test could not be used because there most of the cases had no change in performance, so those cases could not be ranked.

Optimizing both the leaf transmission factor and the rounded leaf offset table results in an average -0.81 ± 1.8 % change in gamma index passing rate, relative to the performance of the default TPS planar dose calculation. Using a paired Student's t test and the Wilcoxon Signed Rank test, p-values were calculated to be 0.00315 and 0.00288 respectively, showing that planar diode IMRT QA passing rates worsened significantly after optimization of leaf transmission at a significance level of $p = 0.05$.

Table 3.3: IMRT QA results comparing various TPS dose calculations to planar diode array measurements. The relative difference refers to the gamma index passing rate of the specified case relative to that of the default TPS calculation.

		Gamma Index Passing Rate (%)				Relative Difference (%)		
Field Index	Site	Default	Offset Only	Trans Only	Trans + Offset	Offset Only	Trans Only	Trans + Offset
1	Breast	98.1	98.3	97.5	96.7	0.2	-0.6	-1.4
2	“	94.5	94.6	88.4	91.0	0.1	-6.5	-3.7
3	“	96.6	97.0	95.0	95.2	0.4	-1.7	-1.4
4	“	99.2	98.9	97.4	98.1	-0.3	-1.8	-1.1
5	“	93.0	93.2	92.2	92.7	0.2	-0.9	-0.3
6	“	96.6	96.3	96.1	95.9	-0.3	-0.5	-0.7
7	“	96.1	95.9	95.9	95.9	-0.2	-0.2	-0.2
8	“	92.8	92.8	89.9	89.5	0.0	-3.1	-3.6
9	“	90.2	90.2	84.3	86.4	0.0	-6.5	-4.2
10	“	95.6	95.6	93.0	93.5	0.0	-2.7	-2.2
11	Lung	99.5	99.5	98.6	98.6	0.0	-0.9	-0.9
12	“	98.2	98.2	98.3	98.3	0.0	0.1	0.1
13	“	100	100	100	100	0.0	0.0	0.0
14	“	90.4	90.4	84.4	87.1	0.0	-6.6	-3.7
15	“	99.2	99.2	99.2	99.2	0.0	0.0	0.0
16	“	97.8	97.8	97.9	98.4	0.0	0.1	0.6
17	“	100	100	100	100	0.0	0.0	0.0
18	“	100	100	100	100	0.0	0.0	0.0
19	“	100	100	100	100	0.0	0.0	0.0

3.3.2.Film Results

Figure 3.13, Figure 3.14, and Figure 3.15 show gamma index analyses comparing measured film dose distributions compared against default TPS calculations, TPS calculations with optimized transmission, and TPS calculations with both MLC transmission and offset table optimized. Results for these gamma comparisons are 98.5%, 97.5%, and 96.7% respectively. These are generally representative of the film results.

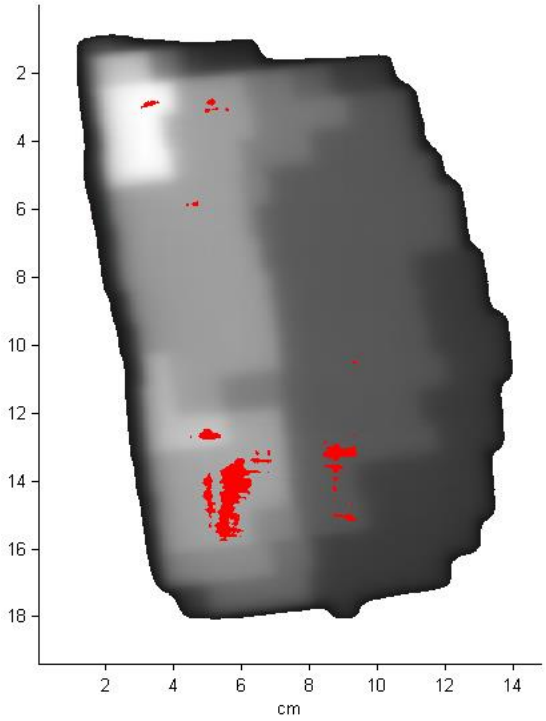

Figure 3.13: Field 1 gamma index comparison between film measurement and TPS calculation with optimized MLC transmission and optimized offset table using clinical gamma index criteria. Passing rate: 98.5%.

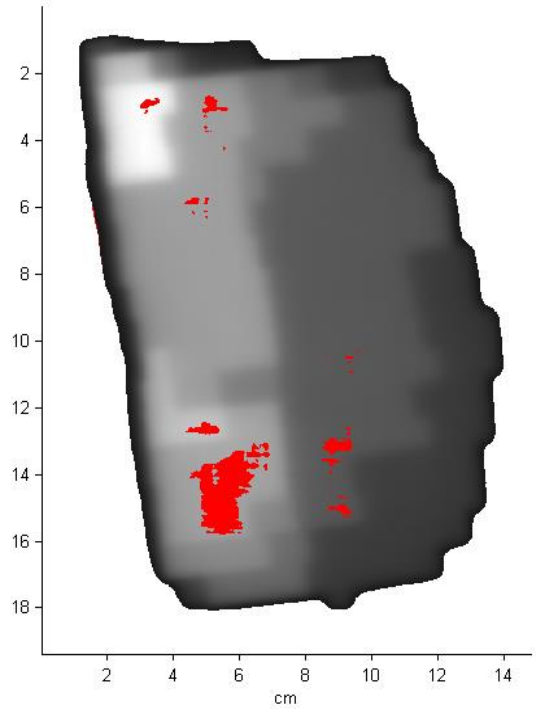

Figure 3.14: Field 1 gamma index comparison between film measurement and TPS calculation with optimized MLC transmission and optimized offset table using clinical gamma index criteria. Passing rate: 97.6%.

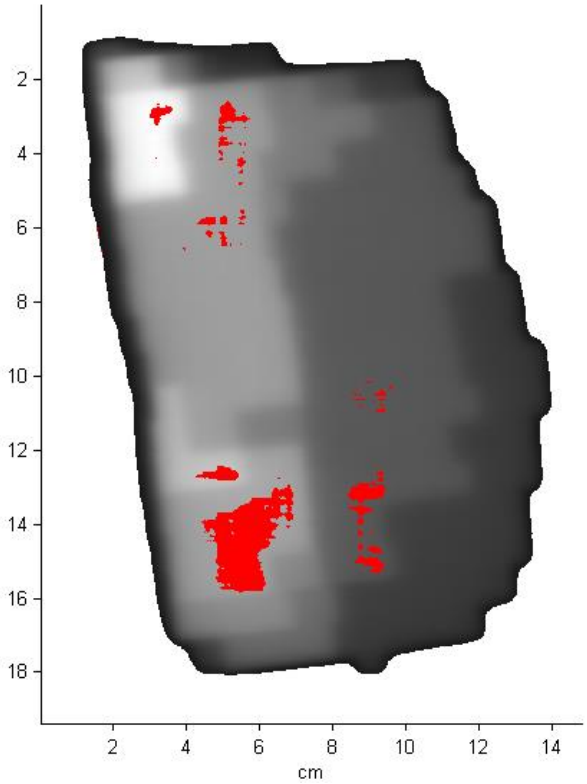

Figure 3.15: Field 1 gamma index comparison between film measurement and TPS calculation with optimized MLC transmission and optimized offset table using clinical gamma index criteria. Passing rate: 96.7%

Table 3.4 contains all gamma index results for film measurements. Optimizing only the leaf transmission factor resulted in an average -1.48 ± 2.1 % change in gamma index passing rate. Using a paired Student's t test and the Wilcoxon Signed Rank test, p-values were calculated to be 0.00695 and 0.00452 respectively, showing that planar diode IMRT QA passing rates worsened significantly after optimization of leaf transmission at a significance level of p = 0.05.

Optimizing the rounded leaf offset table only resulted in an average -0.12 ± 1.3 % change in gamma index passing rate. Using a paired Student's t test and the Wilcoxon Signed Rank test, p-values were calculated to be 0.68406 and

0.72786 respectively, showing that planar diode IMRT QA passing rates were not significantly different at a significance level of p = 0.05.

Table 3.4: IMRT QA results comparing various TPS dose calculations to radiographic film measurements. The relative difference refers to the gamma index passing rate of the specified case relative to that of the default TPS calculation.

		Gamma Index Passing Rate (%)				Relative Difference (%)		
Field Index	Site	Default	Offset Only	Trans Only	Trans + Offset	Offset Only	Trans Only	Trans + Offset
1	Breast	98.52	95.72	97.55	96.72	-2.84	-0.98	-1.83
2	“	78.50	78.32	77.13	77.49	0.06	-1.75	-1.29
3	“	88.68	88.55	88.74	88.38	-0.15	0.07	-0.34
4	“	93.24	92.62	92.25	92.35	-0.66	-1.06	-0.95
5	“	89.35	89.38	89.36	91.59	0.03	0.01	2.51
6	“	96.77	96.74	96.10	96.76	-0.03	-0.69	-0.01
7	“	83.07	81.11	81.64	81.05	-1.16	-1.72	-2.43
8	“	92.59	93.99	89.43	90.59	1.51	-3.41	-2.16
9	“	90.42	90.30	87.25	88.83	-0.13	-3.51	-1.76
10	“	90.43	91.08	88.06	90.08	0.72	-2.62	-0.39
11	Lung	99.78	99.94	98.55	99.14	0.16	-1.23	-0.64
12	“	95.08	95.75	95.75	95.12	0.70	0.70	0.04
13	“	99.97	99.99	99.77	99.96	0.02	-0.20	-0.01
14	“	93.17	94.93	85.99	88.37	1.89	-7.71	-5.15
15	“	99.35	99.73	99.36	99.53	0.38	0.01	0.18
16	“	98.30	98.83	95.53	96.00	0.54	-2.82	-2.34
17	“	79.95	77.19	81.83	82.53	-3.45	2.35	3.23
18	“	88.48	89.01	86.01	87.23	0.60	-2.79	-1.41
19	“	95.07	94.59	94.29	94.49	-0.50	-0.82	-0.61

Optimizing both the leaf transmission factor and the rounded leaf offset table resulted in an average -0.81 ± 1.8 % change in gamma index passing rate, relative to the performance of the default TPS planar dose calculation. Using a paired Student’s t test and the Wilcoxon Signed Rank test, p-values were

calculated to be 0.06723 and 0.03026 respectively, a split result that shows an inconclusive statistical significance a significance level of p = 0.05.

3.3.3.Compiled Results

Figure 3.16, Figure 3.17, and Figure 3.18 show graphical box plot representations of the gamma index performance for cases with optimized leaf transmission factor only, optimized rounded leaf offset table only, and with both leaf transmission factor and offset tables results tabulated in Table 3.3 and Table 3.4.

The results in Figure 3.16 indicate that optimizing only the leaf transmission factor results in a decrease in gamma index passing percentage. The middle two quartiles of the 19 analyzed fields all show a worsening of performance of between 0 to -2.27 % for planar diode array measurements and -0.10 and -2.71 % for radiographic film measurements. Both measurement modalities show similar results, although the film measurements show a greater variance than planar diode array measurements.

Figure 3.17 reveals little change in gamma index pass rate after optimizing the only the rounded leaf offset table. 12 of the 19 fields measured via planar diode array showed no change at all in the gamma index passing rate. For film measurements, the median change in gamma index performance was 0.034%, and the middle two quartiles of the analyzed fields showed a change in performance between 0.60 to -0.33 %.

Figure 3.18 reveals that optimizing both the rounded leaf offset table and the leaf transmission factor resulted in a slight worsening of gamma index

performance. planar diode array measurements showed a median change in passing rate of -0.725 %, with the two middle quartiles showing a change in passing rate of between 0 to -1.82 %. Radiographic film measurements showed a median change in passing rate of -0.641 %, with the two middle quartiles showing a change in passing rate between -0.01 to -1.79 %.

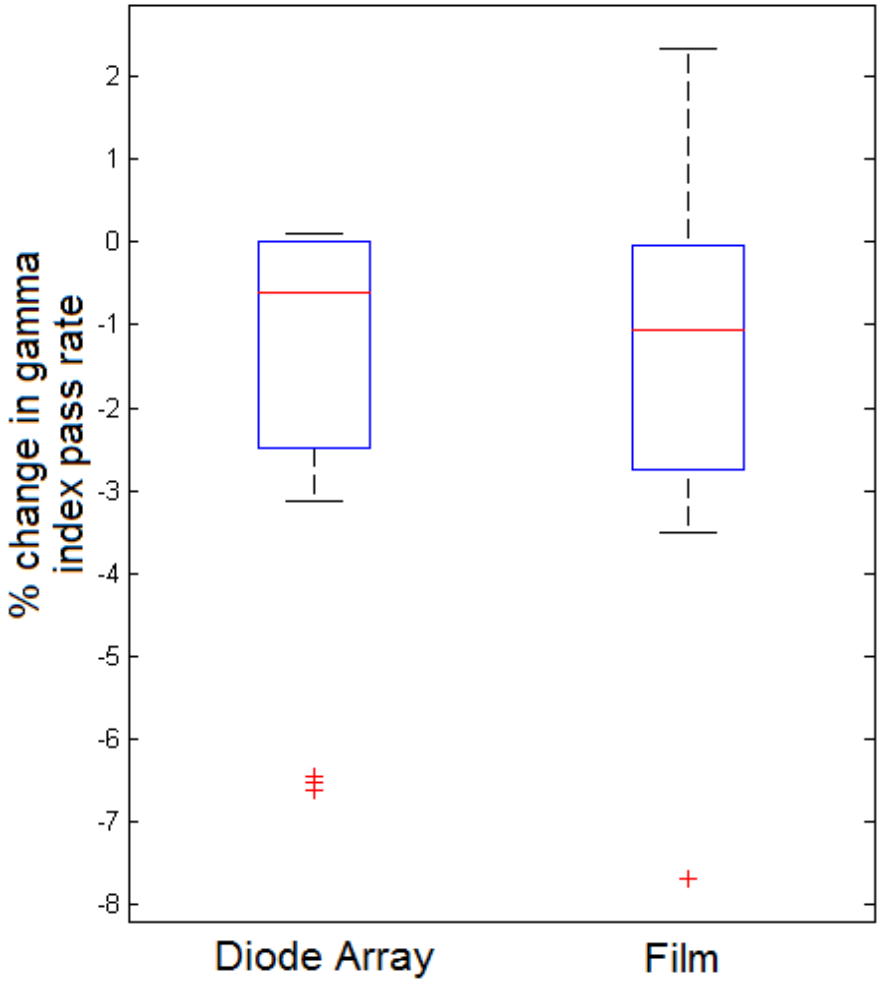

Figure 3.16: Changes in gamma index performance after optimizing only the leaf transmission factor, relative to gamma index performance of the default TPS model. The red line represents the median, the blue box contains the middle two quartiles, and the black lines contain the upper and lower quartiles. Outliers are shown as red plus signs.

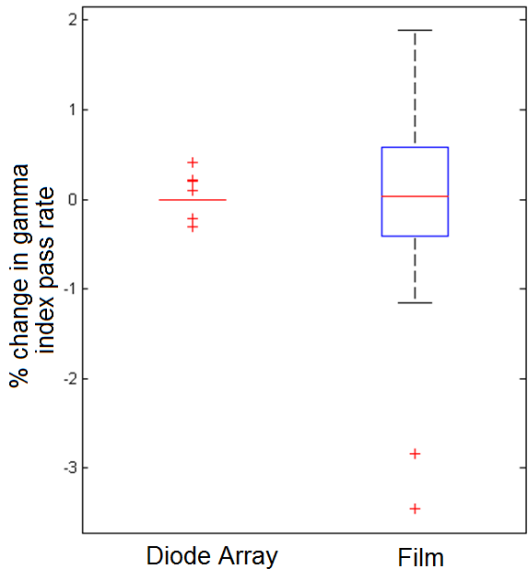

Figure 3.17: Changes in gamma index performance after optimizing only the rounded leaf offset table, relative to gamma index performance of the default TPS model. The red line represents the median, the blue box contains the middle two quartiles, and the black lines contain the upper and lower quartiles. Outliers are shown as red plus signs. For the planar diode array results, optimizing the offset table resulted in no change in gamma index performance for 12 of 19 IMRT plans.

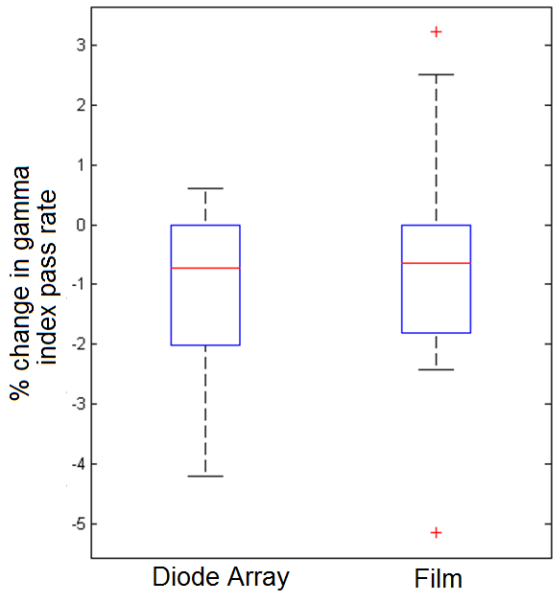

Figure 3.18: Changes in gamma index performance after optimizing both the leaf transmission factor and the rounded leaf offset table, relative to gamma index performance of the default TPS model. The red line represents the median, the blue box contains the middle two quartiles, and the black lines contain the upper and lower quartiles. Outliers are shown as red plus signs.

3.4.Significance of Other TPS Parameters

This section contains results after remodeling the beam to demonstrate that other parameters in the TPS are more responsible for the fit at a depth of 5 cm. The various changes made to the TPS include the reduction in scatter from the flattening filter, a reduction in the effective source size, a slight increase in fluence from the flattening filter, and both the leaf transmission and rounded leaf offset table optimizations.

3.4.1.Picket Fence Test Results

Figure 3.19 shows the picket fence test results. Gafchromic film profile measurement is compared to the default TPS and remodeled TPS dose profile calculations. Excellent agreement is seen between the measured film profile and the TPS calculation with various parameters remodeled as described in Section 2.3.4.

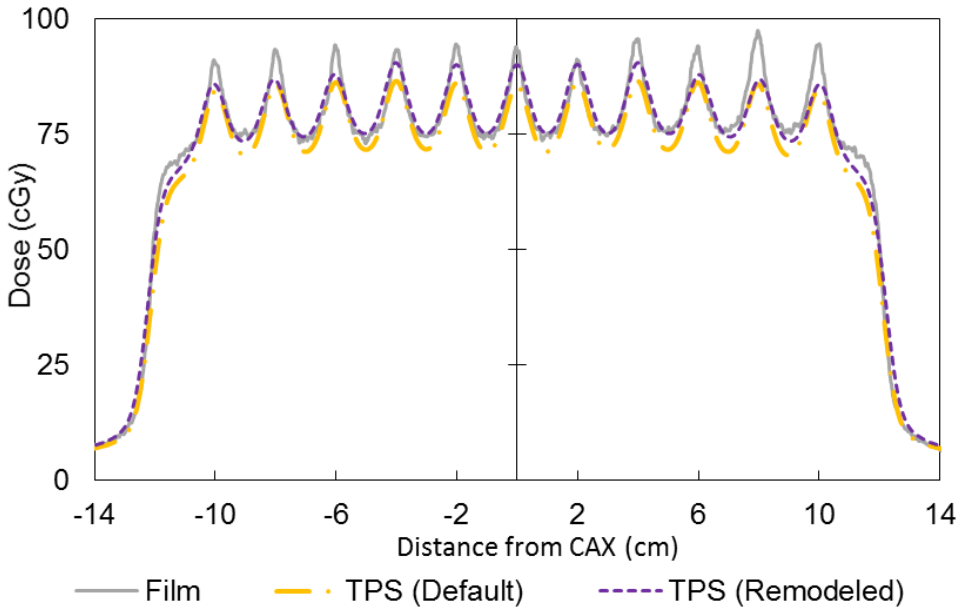

Figure 3.19: Picket fence comparison with remodeled beam.

3.4.2.IMRT QA Results

Table 3.5 and Table 3.6 contain all gamma index results comparing the remodeled beam to both planar diode array and EDR2 radiographic film measurements respectively.

Table 3.5: IMRT QA results comparing various TPS dose calculations to planar diode array measurements. The relative difference refers to the gamma index passing rate of the remodeled beam relative to that of the default TPS calculation.

		Gamma Index Passing Rate (%)		Relative Difference (%)
Field Index	Treatment Site	Default	Remodeled	Remodeled
1	Breast	98.1	98.1	0.0
2	“	94.5	95.2	0.7
3	“	96.6	95.4	-1.2
4	“	99.2	99.7	0.5
5	“	93	98.7	6.1
6	“	96.6	98.6	2.1
7	“	96.1	98.6	2.6
8	“	92.8	96.1	3.6
9	“	90.2	93	3.1
10	“	95.6	97.2	1.7
11	Lung	99.5	99.5	0.0
12	“	98.2	98.2	0.0
13	“	100	100	0.0
14	“	90.4	91.8	1.5
15	“	99.2	99.2	0.0
16	“	97.8	98.9	1.1
17	“	100	100	0.0
18	“	100	100	0.0
19	“	100	100	0.0

Remodeling the beam showed an average 1.15 ± 1.7 % improvement in gamma index passing rate when comparing TPS calculations to planar diode array measurements. Using a paired Student’s t test and the Wilcoxon Signed Rank test, p-values were calculated to be 0.25350 and 0.00988 respectively, a

split result that shows an inconclusive statistical significance a significance level of p = 0.05. The Wilcoxon Signed Rank test shows a significant difference because many of the cases have no change in performance, and these cases must be thrown out because they can't be ranked.

Table 3.6: IMRT QA results comparing various TPS dose calculations to EDR2 radiographic film measurements. The relative difference refers to the gamma index passing rate of the remodeled beam relative to that of the default TPS.

		Gamma Index Passing Rate (%)		Relative Difference (%)
Field Index	Treatment Site	Default	Remodeled	Remodeled
1	Breast	96.07	97.37	1.35
2	"	78.5	77.78	-0.92
3	"	88.68	83.74	-5.57
4	"	93.24	89.93	-3.55
5	"	89.35	90.94	1.78
6	"	96.77	97.7	0.96
7	"	83.07	93.06	12.03
8	"	92.59	98.33	6.20
9	"	90.42	89.84	-0.64
10	"	90.43	91.5	1.18
11	Lung	99.78	99.92	0.14
12	"	95.08	97.68	2.73
13	"	99.97	99.62	-0.35
14	"	93.17	99.52	6.82
15	"	99.35	99.53	0.18
16	"	98.3	98.03	-0.27
17	"	79.95	90.52	13.22
18	"	88.48	90.08	1.81
19	"	95.07	97.17	2.21

Using film, remodeling the beam showed an average 2.07 ± 4.7 % improvement in gamma index passing rate when comparing TPS calculations to radiographic film measurements. According to the paired Student's t test and the Wilcoxon Signed Rank test, p-values were calculated to be 0.63710 and

0.053668 respectively, showing that planar diode IMRT QA passing rates were not significantly different at a significance level of p = 0.05.

Figure 3.20 shows the distribution of change in gamma index passing rate after the beam was remodeled as measured by both the planar diode array and film.

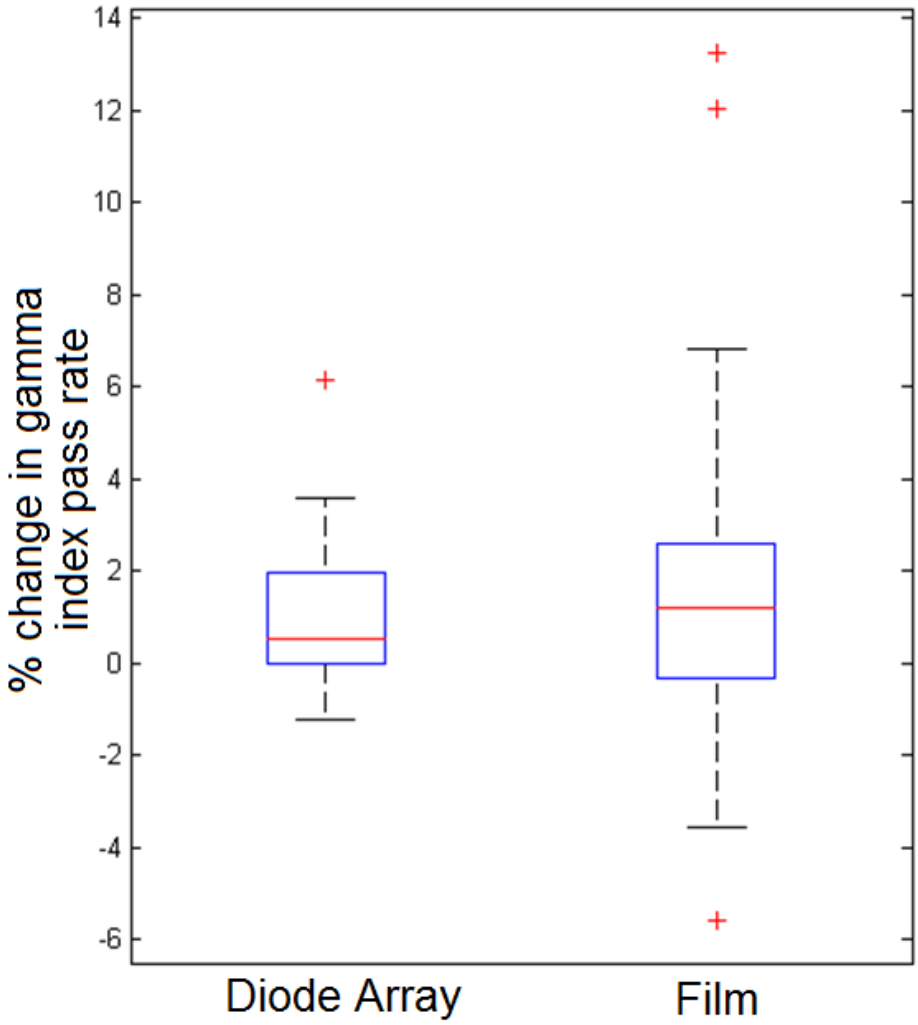

Figure 3.20: Changes in gamma index performance after remodeling the beam, relative to gamma index performance of the default TPS model. The red line represents the median, the blue box contains the middle two quartiles, and the black lines contain the upper and lower quartiles. Outliers are shown as red plus signs.

3.5.Utility of Picket Fence Test Results

Ultimately, the utility of the picket fence test was limited in this study by the dosimeter used to originally commission the machine. The linac was originally commissioned in 2008, using commissioning data measured with a CC13 ionization chamber. Although the CC13 has a relatively small sensitive volume for an ion chamber, there is still a significant dose volume averaging effect. Figure 3.21 shows a profile of a field edge measured with both the CC13 and a diode detector, as measured by physics at MBPCC. In low dose gradient regions, the two detectors agree very well, but as the dose gradient increases, the dose volume averaging effect of the ion chamber becomes apparent. The apparent penumbra width is significantly wider as measured by the CC13 than the penumbra width as measured by the diode. The “shoulder” region (i.e. the open-field area at the edge of the penumbra) is significantly lower and the “tail” region (the out-of-field area near the edge of the penumbra) is significantly higher.

Since the commissioning data was measured with the CC13, the current clinical TPS model parameters were chosen to match the CC13 measured penumbra shape. For this reason, the widened penumbra shape is included in the current clinical model, including the lower shoulder region and the higher tail region. Because the picket fence test overlap regions essentially consist of abutted shoulder regions from multiple segments, the current clinical model underestimates the dose in these regions (Figure 3.3). Optimizing the leaf transmission value and the rounded leaf offset table has a limited effect on the shoulder shape, so calculated dose distributions still demonstrate lower dose in

the overlap region (Figure 3.3 and Figure 3.8). The dose averaging effect means that the apparent source size is significantly larger than it physically is. Accounting for this effect would require remeasuring the commissioning data for a large number of depths, field sizes, and field shapes, which is outside the scope of this work.

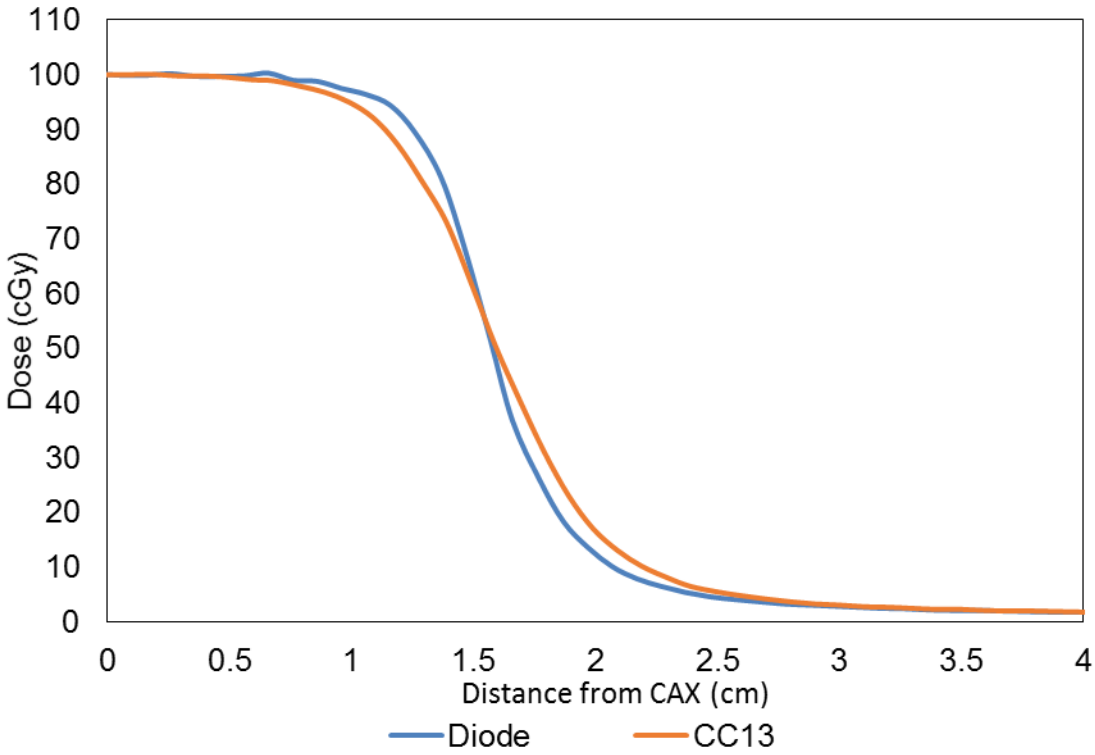

Figure 3.21: A penumbra measured with both diode and CC13 ion chamber. Measurement performed by Dan Neck.

Chapter 4: Discussion

The hypothesis of this project was that improve overall dosimetric accuracy of IMRT plans as calculated by the TPS could be improved by optimizing the rounded leaf offset table and the parameters governing the MLC transmission. This hypothesis was not supported by the results. Optimizing the rounded leaf offset table did not have a significant effect on IMRT gamma index passing rate. Optimizing the leaf transmission factor resulted in a significant worsening of IMRT gamma index passing rate.

4.1.MLC Transmission

It is clear from this study that the default leaf transmission factor currently used in the treatment planning system significantly underestimated the transmission through the MLC. The current leaf transmission factor, 0.001, is the minimum allowed value in the TPS. When the TPS was originally commissioned in 2008, there was a discussion about how this parameter should be determined. Ultimately, it was left to TPS's automatic beam modeling sequence to find the parameters using measured commissioning data. We confirmed that the automodeling sequence would set the leaf transmission factor to 0.001 based on the provided measured data. Although this is not an empirically derived parameter, the TPS adjusted the apparent dose in the tail regions by increasing the scattered radiation dose from the flattening filter. This resulted in a relatively good fit at all field sizes and depths.

However, the film measurements did illuminate several characteristics of the MLC transmission. See Figure 4.1 for a more detailed view of MLC

transmission. The film shows that there is significant interleaf leakage underneath each tongue-and-groove space (Point 1 in Figure 4.1). The magnitude of each interleaf leakage peak also shows a significant amount of variability. It is assumed that the variation in the amount of interleaf leakage is due to variation in the spaces between adjacent leaves. If two leaves are closer together than average, it would result in a smaller interleaf gap, and therefore a smaller amount of radiation would be transmitted through the interleaf space with reduced attenuation, resulting in a smaller amount of interleaf leakage radiation.

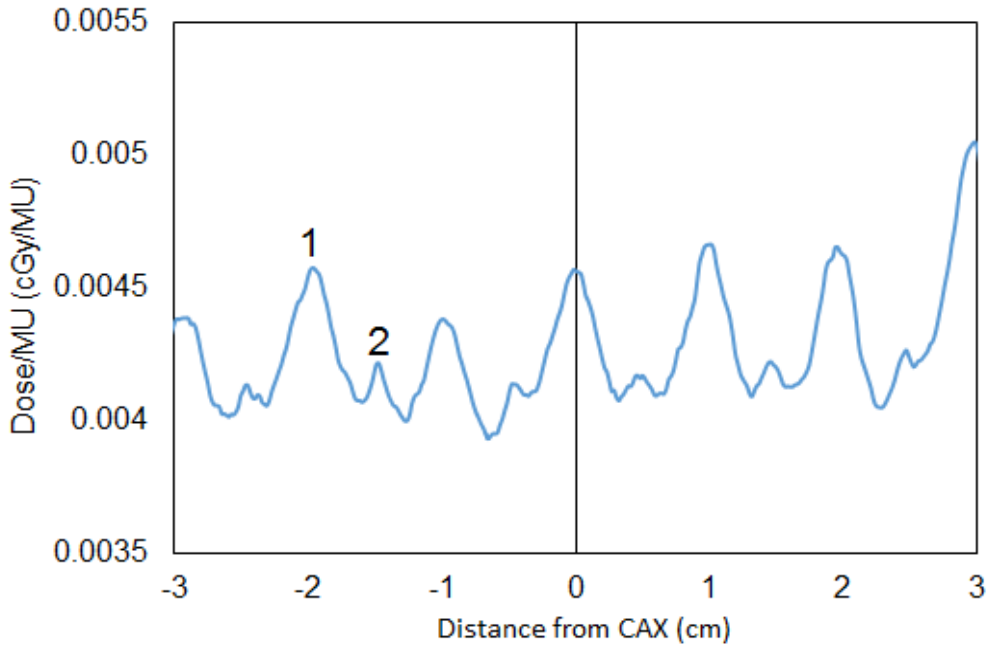

Figure 4.1: Detail of MLC transmission profile. Point 1 is an interleaf leakage peak. Point 2 is a “mini-peak.”

Additionally, smaller radiation peaks were seen between interleaf leakage peaks (Point 2 in Figure 4.1). These smaller peaks were located nearly underneath the middle of each leaf. This could be occurring due to the uneven top and bottom of each leaf. Depending on the angle of incidence, radiation can

miss the interleaf space but still be attenuated less because they miss the thicker parts of the top and bottom of the leaf. See Figure 4.2 for an illustration.

The default TPS configuration has the tongue-and-groove width set to 0 cm. This parameter is physically correct because the Elekta MLCi2 does not have a tongue-and-groove design. However, setting the tongue-and-groove width parameter to 0 cm makes the TPS treat the MLC as a continuous slab, which results in the dose calculation remaining flat across the entire leaf bank. In reality, there are significant peaks seen directly underneath the interleaf spaces.

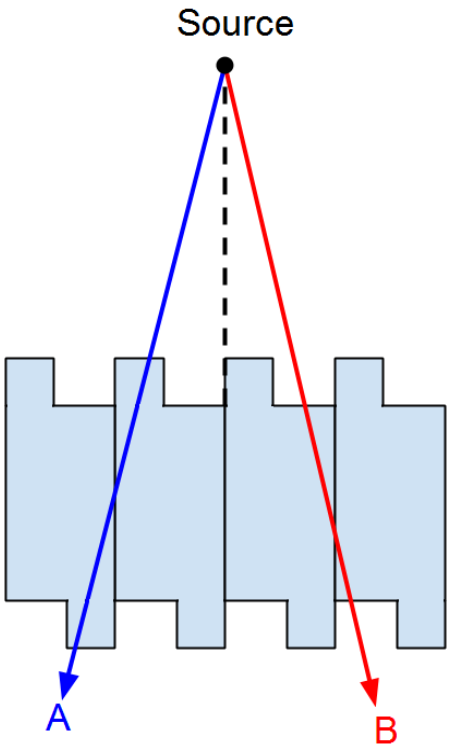

Figure 4.2: Possible explanation of “mini-peaks.” Ray B is attenuated through less material than Ray A because of its angle of incidence, resulting in a larger transmission peak. The geometry of the leaf is exaggerated to demonstrate this effect.

Ultimately, only the leaf transmission component of MLC transmission was optimized. The other component of MLC transmission, interleaf leakage, was not optimized in this work. There were several reasons for this. First, there is a large

variation in the magnitude of the interleaf peaks. Pinnacle^3 provides no way of modeling this variation. Applying a nonzero tongue-and-groove width parameter and an additional interleaf transmission parameter to the treatment planning system would result in dose calculations with a steady, sinusoidal interleaf leakage pattern with constant dose values in the peaks and valleys. The actual interleaf leakage pattern is not consistent as shown in Figure 3.1.

Additionally, Task Group Report 50 recommends averaging the dose over a wide area to measure MLC transmission (Boyer et al., 2001). They recommend using film and taking measurements at several different locations, or using an ion chamber with a large sensitive volume and therefore a large dose averaging effect. It would be difficult to independently measure the radiation transmission through the thickness of the leaf and the interleaf leakage because the additional fluence through the interleaf space will scatter into the spaces directly underneath each leaf. In fact, many commercial TPS do not even model interleaf leakage (Williams & Metcalfe, 2006).

Pasquino et al. (2006) measured the transmission through the MLC of a different Elekta MLC model. Using a Farmer chamber, the transmission measurements included contributions of transmission through the full thickness of the leaf and interleaf leakage (Pasquino et al., 2006). Pasquino et al. reported the averaged leaf transmission to be 0.019 (Pasquino et al., 2006). Their paper did not investigate changes to the TPS.

Garcia-Garduno et al. (2008) measured the transmission through a micro-MLC system. They used radiochromic film because of its energy independent

response (Garcia-Garduno et al., 2008). Garcia-Garduno et al. did distinguish between leaf transmission and additional interleaf leakage, and measured them to be 0.93 ± 0.05 % and 1.08 ± 0.08 % respectively (Garcia-Garduno et al., 2008).

Williams & Metcalfe (2006) investigated the leaf transmission parameter in Pinnacle^3 for a Varian Millenium MLC system. They did not measure the leaf transmission directly, but instead set the transmission parameter based on the performance of a picket fence test (Williams & Metcalfe, 2006). They set the leaf transmission factor to 0.015, because it resulted in the best picket fence performance (Williams & Metcalfe, 2006).

Lafond et al. (2013) investigated the performance of the Elekta MLCi2 for VMAT treatments, and reported the transmission through the MLC to be 0.006, very similar to our chosen leaf transmission value of 0.005.

4.2.Rounded Leaf Offset Table

In the process of optimizing the leaf offset table, a comparison is made to TPS calculated and measured field edge positions. The TPS calculated field edge position is very sensitive to how radiation is attenuated through the rounded tip of the leaf, and is therefore also sensitive to the leaf transmission value used in the TPS. For this reason, we optimized the rounded leaf offset table under two conditions: with the default leaf transmission factor of 0.001 and with the optimized leaf transmission factor of 0.005.

One interesting feature of the optimized offset table is how the slope of the offset table drops at large leaf positions, i.e. when the leaf tip is more than ~16

cm retracted from the central axis or ~-10 cm extended past the central axis. At these leaf positions, the offset remains constant. This shape is endemic to the field edges as calculated by Pinnacle^3. John Rice performed a similar rounded leaf offset optimization in his 2014 paper, and found the same effect (Rice, 2014). It is unclear what exactly is causing this effect, but that question is outside the scope of this work.

There is limited user access to the systems that could calibrate the mechanical leaf positions on the Elekta Synergy linear accelerator to agree with the default TPS offset table. There are only two parameters to calibrate a leaf bank at all possible leaf positions: a slope parameter and an intercept parameter. Our results confirmed that Mary Bird Perkins Cancer Center physics staff did an excellent job of calibrating the linac leaf positions, as illustrated by the fact that the optimized rounded leaf offset table is very similar to the current offset table used in the treatment planning system (Figure 3.5).

When leaf calibrations are performed, usually a variety of IMRT plans are performed and compared to TPS calculated dose distributions (Perrin & Neck, 2015). Each leaf bank is calibrated to maximize performance of these plans. In addition, the tips of the leaf banks are measured with the EPID panels at several different positions to ensure the leaf positions do not drift over time (Perrin & Neck, 2015). The quality of MBPCC's leaf calibration protocol is reflected in our results, which shows that square field sizes between 5 cm and 25 cm have nearly perfect radiological field edge positions. There is minor room for improvement at negative leaf positions (when the leaf is extended past the

central axis). The optimized offset table improves most negative leaf positions by less than 1 mm. In fact, the magnitude of the difference was less than 1 mm for all leaf positions analyzed except for leaf positions of -12 cm, 19 cm, and 20 cm, the three most extreme leaf positions. These leaf positions are rarely seen in IMRT treatments. The averaging difference between default and optimized offset table was -0.2 ± 0.7 mm

Furthermore, the measured profiles used to optimize the rounded leaf offset table were scanned with the spherical 0.13 cm^3 ionization chamber. The rounded leaf offset values range from about 1 mm to about -6 mm, so the 6.0 mm ion chamber diameter is extremely significant in determining the penumbra width. See Section 4.3 and Figure A.1 for more information about the effects of ion chamber dose averaging effects.

Rice (2014) used a similar method to optimize the rounded leaf offset table of the MLCi2 in the Philips Pinnacle^3 TPS. Rice's offset table is significantly different than the optimized offset table developed in this work. The reason for this is the difference in linear accelerator MLC calibration protocol. At MBPCC, the MLC positions are calibrated to maximize radiological agreement between measurements and TPS dose calculations. This is the reason that the optimized offset table is not very different from the currently used offset table. The linac Rice used in his paper was calibrated such that the radiation field edge locations would be coincident with the defined leaf position. That is to say, if the linac was ordered to place the leaf bank position at 5 cm, the leaf would be moved to a position such that the radiological field edge would fall at 5 cm from the central

axis. This leaf calibration protocol has nothing to do with TPS calculations, which is why Rice's optimized TPS table ends up being significantly different than the light field offset table that comes default in Pinnacle^3 for the MLCi2 treatment head.

4.3.Picket Fence Test

The picket fence test is generally considered an excellent test of the field edge position (Rice, 2014), as well as the accuracy of the leaf transmission factor (Williams & Metcalfe, 2006). There are multiple versions of the picket fence test, but the one used in this work consisted of multiple 2.2 cm wide fields which overlapped one another (Rice, 2014). The overlapped regions were planned to be 2 mm wide in the treatment planning system, but since the exact penumbra location is dependent on the offset table and leaf transmission, the actual shape of the overlap region is variable and has a dependence on leaf position. This is the reason the picket fence test should be sensitive to the TPS optimizations carried out in this work. Figure 2.3 shows two adjacent segments of the picket fence test and their cumulative dose.

Optimizing the leaf transmission factor in the TPS from the current clinical value of 0.001 to 0.005 resulted in significant improvement of TPS agreement to the measured picket fence test results (Figure 3.3).

Optimizing only the offset table results in almost no change in picket fence test performance over the default TPS configuration. Overlap regions centered at ± 8 cm perform slightly worse, while overlap regions centered at ± 6 cm perform slightly better.

Optimizing both the leaf transmission factor and the rounded leaf offset table results in slightly worse performance (according to the mean peak-to-valley ratio) than the case with only the transmission optimized and default rounded leaf offset table. The trough regions of the picket fence test are still significantly improved over the default TPS, but the dose in the overlap areas are lower than the case with only the transmission optimized, especially in overlap regions further from the central axis. This happened because the optimized offset table had a larger offset than the default offset table for negative leaf positions when the leaf was past the central axis (Figure 3.5). A larger offset means the leaf tip is shifted forward for the purposes of dose calculations and will induce slightly more shielding of radiation beams, which results in smaller and lower magnitude overlap regions.

4.4.IMRT QA

All of the IMRT QA done in this project was performed at a depth of 5 cm. The film used for IMRT QA was placed under 5 cm of water equivalent plastic and the planar diode array device has the radiological equivalent of 5 cm of water buildup (although the actual physical depth is smaller). At a depth of 5 cm, the current clinical model is already higher in the tail regions (Figure A.1). Optimizing the leaf transmission value to a more physically accurate value of 0.005 makes the agreement in these regions worse than the current clinical model. This is why the IMRT QA gamma index analysis shows worse results with the optimized TPS parameters.

The leaf transmission factor can also affect in-field dose distributions, more so for complex IMRT plans with complicated subfield shapes where parts of the in-field region are covered by MLC at certain times. Conversely, the optimized leaf transmission value of 0.005 is relatively insignificant compared to an open field dose, especially when analyzing dose distribution accuracy with a 3% dose difference criteria.

Optimizing the rounded leaf offset table also had a relatively small effect on gamma index analysis pass rates. For the most part, the optimized offset table is very similar to the current clinical offset table (Figure 3.5). At the most retracted leaf positions there is an improvement in the leaf offset of > 1 mm, but these retracted leaf positions are relatively rare. Most IMRT plans are closer to the center of the field, so the improvement at these leaf positions has little effect on the IMRT results shown in this work.

The beam was remodeled to demonstrate that IMRT QA results would be more sensitive to other TPS parameters. Various parameters were changed, resulting in a slight improvement in gamma index analysis passing rate. Since all the IMRT QA measurements were done at a depth of 5 cm, the changes made were specifically chosen to improve agreement at this depth. In reality, one must consider the performance of the TPS model at all depths and field sizes. The various changes made while remodeling the 6 MV beam (as described in Section 2.3.4) resulted in an excellent agreement between the measured data and the calculated TPS model (Figure A.1). The change which was most responsible for the improvement in IMRT QA performance was a reduction in the scatter from

the flattening filter. However, these improvements should not be adopted for clinical use because the remodeled parameters are not based on any physical measurements and because the performance of the TPS at other depths is also important. Figure A.2 shows commissioning data compared to the default clinical model and the remodeled beam. The remodeled beam shows significantly worse performance at this depth and field size. It would be better to allow Pinnacle^{3}'s automodeling sequence to account for the measured data at all field sizes and depths.

4.5.Implication and Significance

Accuracy of treatment planning system dose calculations is extremely important. The dose inside the planning treatment volume must be known so that an adequate prescription can be made (Boyer et al., 2001). Without an accurate treatment planning system, dose could be underestimated in the planning treatment volume, leading to a failure of local tumor control. Similarly, dose outside the planning treatment volume is also very important (Boyer et al., 2001). The treatment planning system must be accurate to adequately understand risk to healthy tissue and critical structures in the patient.

Intensity Modulated Radiation Therapy QA at MBPCC performs very well for most cases. There is not a significant amount of IMRT QA that exceeds the MBPCC intervention criteria. MBPCC procedures state that a patient can be treated with IMRT if their patient-specific IMRT QA determines that 90% of evaluated points pass gamma index analysis with the criteria of 3 mm distance-to-agreement and 3 % dose difference. However, in nearly all cases the actual

criteria used is that 95% of points must pass the criteria of 3 mm distance-to-agreement and 3 % dose difference. If a patient's IMRT QA fails to pass these more stringent IMRT QA parameters, the treatment is usually replanned or remeasured. This rarely happens.

This work has shown that the rounded leaf offset table in the treatment planning system is not a significant source of inaccuracy in treatment planning system dose calculations, despite the fact that the rounded leaf offset table in the TPS has never been changed from its default value. This also demonstrates that MBPCC's linac leaf calibration protocol is adequate, despite the fact that Elekta linear accelerators offer limited capability to affect leaf position calibration.

This work also demonstrated that the current TPS model significantly underestimates the transmission through the MLC (including leaf transmission and interleaf leakage), but this does not negatively impact the TPS performance at calculating patients' IMRT plans due to the fact the current TPS model already overestimates dose at a depth of 5 cm in water. Additionally, the dose in the out-of-field regions has a relatively small effect on overall gamma index passing rate because measured dose points that are lower than 10 % of the maximum planar dose are not analyzed, specifically because the out-of-field region is known have lower dosimetric accuracy (Perrin & Neck, 2015).

To demonstrate the sensitivity of TPS performance to other parameters, the additional work of remodeling the 6 MV beam to optimize the fit between the TPS model and measured commissioning data was performed. This was achieved by making additional alterations to the parameters controlling scatter

from the flattening filter, the source size, and the fluence through the flattening filter (Section 2.3.4). This resulted in improved TPS performance of the 19 IMRT plans analyzed (relative to the default TPS configuration) as determined by gamma index analysis. This result demonstrates that these other parameters besides leaf transmission and rounded leaf offset are more responsible for the quality of the fit at this depth. However, the quality of a TPS model must be evaluated at many different field sizes and depths, which is why measured data must be collected under a wide variety of conditions to commission a machine. In fact, the remodeled beam shown in this work should not be used for clinical dose calculations because it actually makes the TPS conform worse to measured commissioning data at deeper depths and larger field sizes (Figure A.2). This demonstrates that the quality of the TPS model is more complicated than the fit under any one individual condition.

The current clinical TPS parameter for leaf transmission is not physically accurate, but the complete model for the 6 MV beam works very well at a variety of depths and field sizes. Changing the leaf transmission factor to a more physically accurate value causes TPS dosimetric accuracy to worsen. This work has demonstrated that the MLC transmission and rounded leaf offset do not need to be adjusted in the TPS to improve TPS performance. Due to the many different possible linear accelerators, treatment planning systems, and clinical calibration protocols, the results shown here do not necessarily apply to other clinics. However, different clinics may have the same questions about the accuracy of their TPS regarding MLC transmission and rounded leaf offset. The

methods set forth in this work can be adapted to investigate these factors for other TPSs and linacs.

4.6.Strengths and Limitations

The main strength of this work is that it demonstrates that the rounded leaf offset table and the MLC transmission are not significant sources of inaccuracy in MBPCC's current TPS dose calculations for treatment delivered by linacs equipped with the Elekta MLCi2. These TPS parameters do not have to be further investigated to improve TPS performance.

However, the main limitation of this work is that it is fairly limited in scope. This project only investigated the performance of linacs with the Elekta MLCi2 treatment head, as calculated by Philips Pinnacle^3 TPS. The conclusions reached don't necessarily apply to other linacs or treatment planning systems, although the procedures used to explore the rounded leaf offset table and MLC transmission could be extended to other linacs. With different linacs and/or treatment planning systems, these TPS parameters could be significant sources of error in dose calculation accuracy.

Furthermore, there are many different ways to calibrate MLC leaf positions, and other techniques might not result in the same quality of agreement between calculated and measured dose distributions. Clinics with different leaf calibration protocols could find that optimizing the rounded leaf offset table does improve TPS performance.

4.7.Future Work

The rounded leaf offset table and MLC transmission factor do not need to be further investigated as ways to improve the performance of MBPCC's TPS dose calculations of treatments delivered by the MLCi2. MBPCC leaf calibration protocol and overall TPS commissioning are excellent. The largest area that could improve the quality of TPS dose calculations probably has to do with the dose averaging effect of the ion chamber originally used to measure commissioning data for linacs equipped with the MLCi2. The machines could be recommissioned by remeasuring this data with a much smaller diode detector to achieve a more accurate penumbra shape in the TPS.

Chapter 5: Conclusion

The goal of this work was to optimize certain parameters governing the modeling of the Elekta MLCi2 treatment head in the Philips Pinnacle^3 treatment planning system, with the ultimate goal of improving the accuracy of calculated IMRT dose distributions. Specifically, the rounded leaf offset table and the MLC transmission parameters were optimized.

The hypothesis was that the dosimetric accuracy of the treatment planning system could be improved by optimizing the parameters in the TPS that govern the MLC transmission and the rounded leaf offset. This was proven false by the fact that gamma index analysis of IMRT plans produced no statistically significant difference in IMRT accuracy after optimizing the rounded leaf offset values, and a statistically significant worsening in IMRT accuracy after optimizing the leaf transmission factor.

Changing the leaf transmission to a more physically accurate value resulted in worse performance as measured by gamma index analysis of IMRT plans. The physical accuracy of any one individual parameter is not as important as the overall dosimetric accuracy of the model, so the TPS should be setup while editing all parameters simultaneously.

References

Berger, M. J., Hubbell, J. H., Seltzer, S. M., Chang, J., Coursey, J. S., Sukumar, R., Zucker, D. S., & Olsen, K. (2009, 2014). XCOM: Photon Cross Sections Database. Retrieved 03/07/2015, 2015, from http://www.nist.gov/pml/data/xcom/.

Boyer, A., Biggs, P., Galvin, J., Klein, E., LoSasso, T., Low, D., Mah, K., & Yu, C. (2001). Basic applications of multileaf collimators: Medical Physics Publishing.

Casanova Borca, V., Pasquino, M., Russo, G., Grosso, P., Cante, D., Sciacero, P., Girelli, G., La Porta, M. R., & Tofani, S. (2012). Dosimetric characterization and use of GAFCHROMIC EBT3 film for IMRT dose verification. Journal of Applied Clinical Medical Physics, 14(2), 4111.

Ezzell, G. A., Galvin, J. M., Low, D., Palta, J. R., Rosen, I., Sharpe, M. B., Xia, P., Xiao, Y., Xing, L., & Yu, C. X. (2003). IMRT commissioning: Multiple institution planning and dosimetry comparisons, a report from AAPM Task Group 119. Medical Physics, 30(8), 2089-2115.

Gafchromic EBT3 Manual. (2011). 1361 Alps Road, Wayne, New Jersey 07470, USA: International Specialty Products.

Garcia-Garduno, O. A., Celis, M. A., Larraga-Gutierrez, J. M., Moreno-Jimenez, S., Martinez-Davalos, A., & Rodriguez-Villafuerte, M. (2008). Radiation transmission, leakage and beam penumbra measurements of a micro-multileaf collimator using GafChromic EBT film. Journal of Applied Clinical Medical Physics, 9(3), 2802.

Hariri, S., & Shahriari, M. (2010). Suggesting a new design for multileaf collimator leaves based on Monte Carlo simulation of two commercial systems. Journal of Applied Clinical Medical Physics, 11(3), 3101.

Lafond, C., Chajon, E., Devillers, A., Louvel, G., Toublanc, S., Olivier, M., Simon, A., De Crevoisier, R., & Manens, J. P. (2013). Impact of MLC leaf width on volumetric-modulated arc therapy planning for head and neck cancers. Journal of Applied Clinical Medical Physics, 14(6), 4074.

Low, D. A., Harms, W. B., Mutic, S., & Purdy, J. A. (1998). A technique for the quantitative evaluation of dose distributions. Medical Physics, 25(5), 656-661.

MapCHECK 2 Manual. (2015). Retrieved from: www.sunnuclear.com/documents/MapCHECK2-3DVH.pdf.

Mohan, R., Chui, C., & Lidofsky, L. (1985). Energy and angular distributions of photons from medical linear accelerators. Medical Physics, 12(5), 592-597.

Orton, R. (2006). LEAF A, MLCi2 SCHEMATIC (3.0 ed.): Elekta AB.

Pai, S., Das, I. J., Dempsey, J. F., Lam, K. L., Losasso, T. J., Olch, A. J., Palta, J. R., Reinstein, L. E., Ritt, D., Wilcox, E. E., & American Association of Physics in, M. (2007). TG-69: radiographic film for megavoltage beam dosimetry. Medical Physics, 34(6), 2228-2258.

Particular requirements for the safety of electron accelerators in the range 1 MeV to 50 MeV. (1998) (2.0 ed.). 3, rue de Varembé Geneva, Switzerland: International Electrotechnical Commission.

Payne, J. (2015). Personal communications.

Perrin, D., & Neck, D. (2015). Personal communications.

Rice, J. R. (2014). Optimization of the rounded leaf offset table in modeling the multileaf collimator leaf edge in a commercial treatment planning system. Journal of Applied Clinical Medical Physics, 15(6), 4899.

Vial, P., Oliver, L., Greer, P. B., & Baldock, C. (2006). An experimental investigation into the radiation field offset of a dynamic multileaf collimator. Physics in Medicine and Biology, 51(21), 5517-5538.

Williams, M. J., & Metcalfe, P. (2006). Verification of a rounded leaf-end MLC model used in a radiotherapy treatment planning system. Physics in Medicine and Biology, 51(4), N65-78.

Appendix A: Commissioning Data

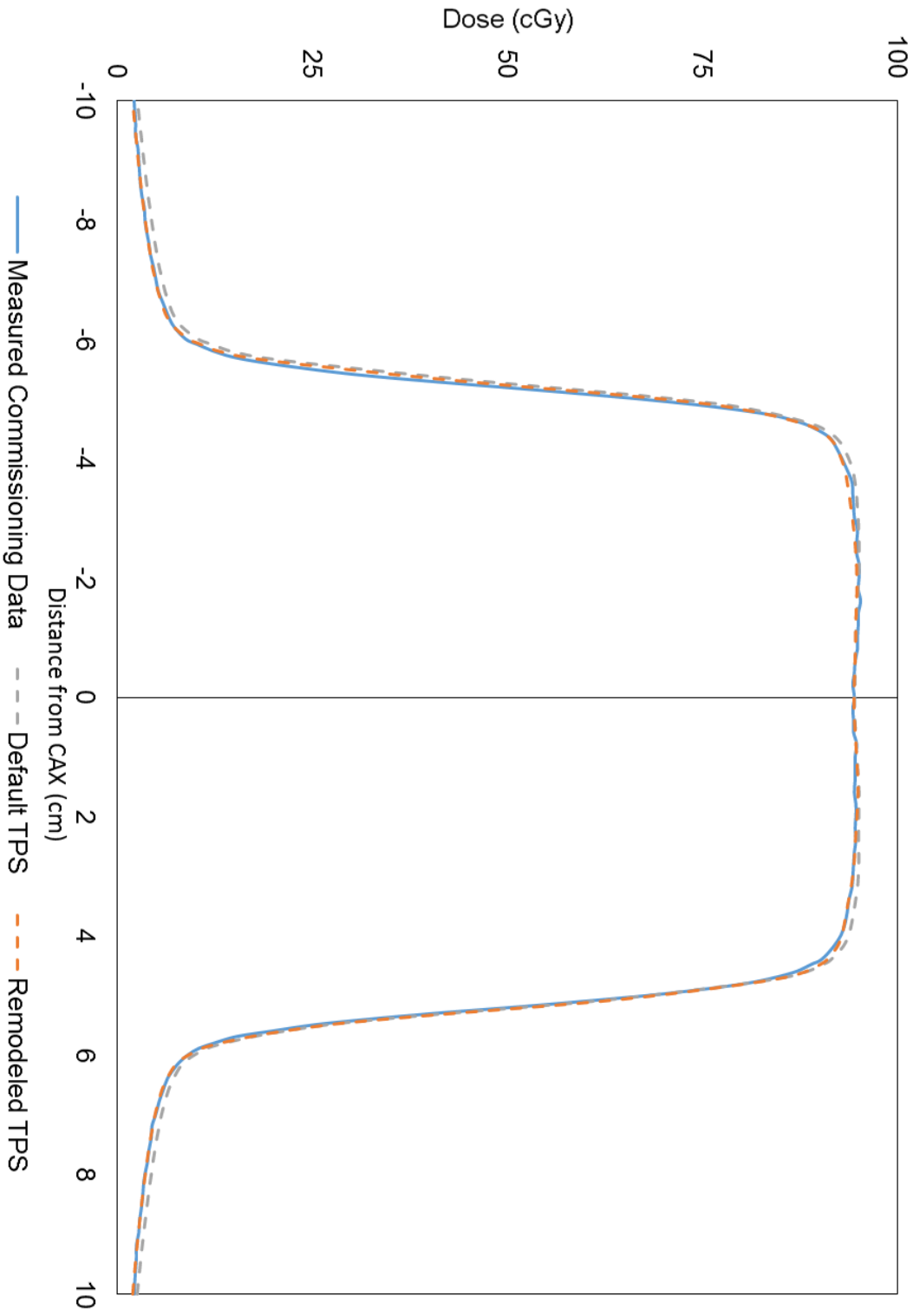

Figure A.1: Default and remodeled TPS dose profiles and measured commissioning data for a 10 cm x 10 cm, d = 5 cm, SSD = 95 cm. Data measurement was performed by Dan Neck in 2008.

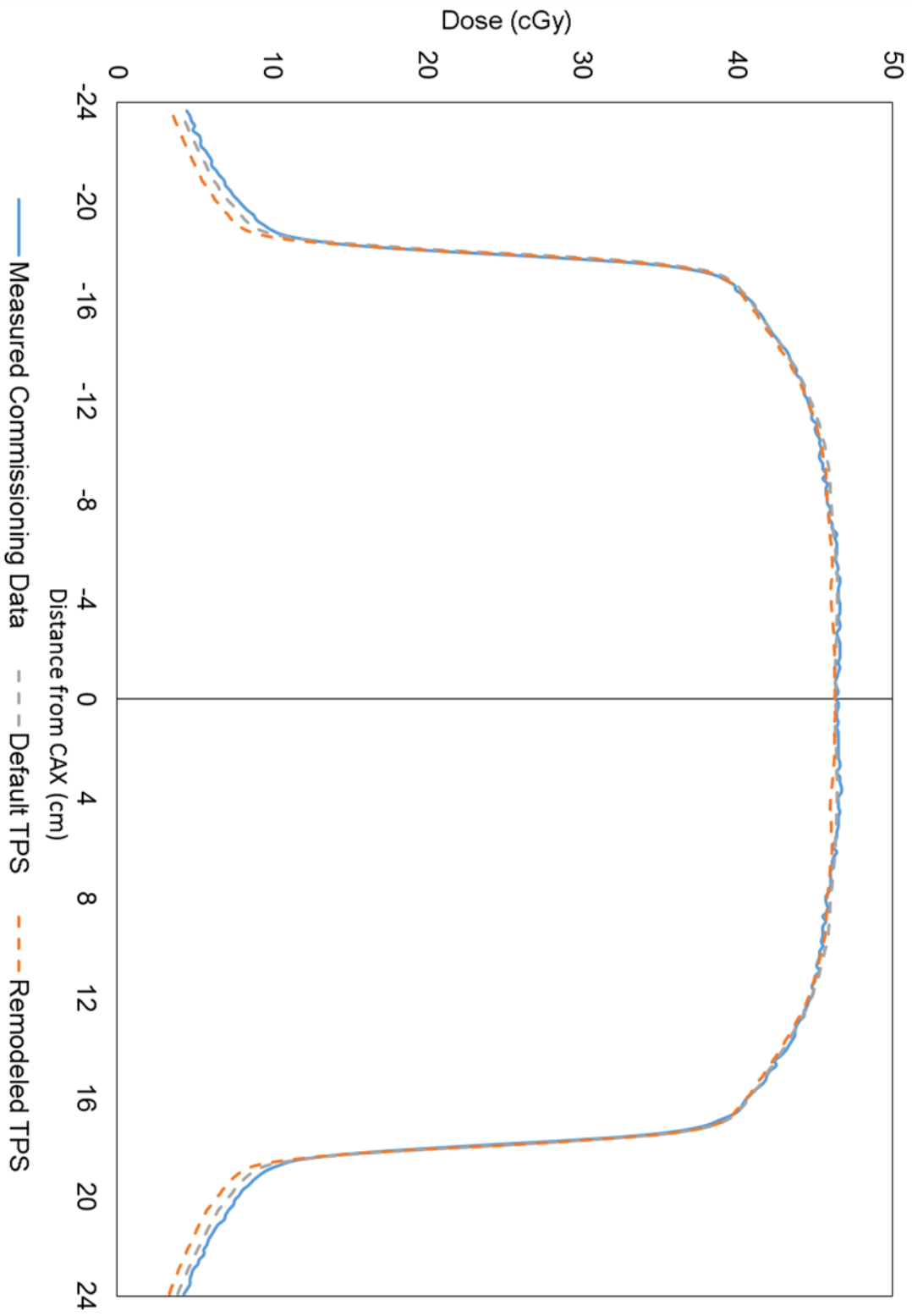

Figure A.2: Default and remodeled TPS dose profiles and measured commissioning data for a 30 cm x 30 cm, d = 20 cm, SSD = 80 cm. Data measurement was performed by Dan Neck in 2008.

Vita

Nicholas Petersen was born in Bend, Oregon in 1988 to his parents, Richard and Marcia Petersen. He has one older brother, Curtis Petersen. After graduating from Summit High School in Bend in 2007, he enrolled at Oregon State University in Corvallis, Oregon. He graduated from OSU with a B.S. in Physics and a B.S. in Engineering Physics in 2012. After graduation, he entered Louisiana State University's Medical Physics program, and moved to Baton Rouge in August of 2012. After completion of his Master of Science degree at LSU, Nick will continue his medical physics education as a resident at Christiana Care Health System in Newark, Delaware. He hopes to eventually work in cancer care as a clinical medical physicist.